Front. Energy 2021, 15(4): 887–915
https://doi.org/10.1007/s11708-021-0789-1

RESEARCH ARTICLE

Sanjeev GUPTA, Martin FREITAG, Gerhard POSS

THAI experimental research on hydrogen risk and source term related safety systems

Abstract In the defense-in-depth concept employed for the safety of nuclear installations, maintaining integrity of containment as the last barrier is of high importance to limit the release of radioactivity to the environment in case of a severe accident. The active and passive safety systems implemented in containments of light water reactors (LWRs) are designed to limit the consequences of such accidents. Assessing the performance and reliability of such systems under accident conditions is critical to the safety of nuclear installations.

In the aftermath of the Fukushima accident, there has been focus on re-examining the existing safety systems to demonstrate their capabilities for a broader range of boundary conditions comprising both the early as well as the late phases of an accident. In addition to the performance testing of safety systems, their interaction with containment atmosphere needs detailed investigations to evaluate the effects of operation of safety systems on H_2 risk and fission product (FP) behavior in containment, which may ultimately have an impact on the source term to the environment.

In this context, an extensive containment safety related experimental research has been conducted in a thermal-hydraulics, hydrogen, aerosols, and iodine test facility (THAI, 60 m^3, single vessel)/(THAI$^+$, 80 m^3, two interconnected vessels). Related to the subject of this paper, experimental investigations covered performance testing of various safety and mitigation systems, i.e., containment spray, passive autocatalytic recombiner (PAR), pressure suppression pool (water pools), and effects of their operation on H_2 risk and in-containment FP behavior. The experimental results have provided a better phenomenological understanding and database for validation and further improvement of a safety analysis tool based on computation fluid dynamic (CFD) and lumped parameter (LP) modeling approach. This paper summarizes the main insights obtained from the aforesaid THAI experimental research covering safety systems installed in containments of LWRs. The relevance of experimental outcomes for reactor safety purpose is also discussed.

Keywords severe accident, containment, safety, mitigation, H_2 risk, source term

1 Introduction

Maintaining containment integrity is of fundamental importance to avoid fission product (FP) release to the environment, which can be seen evidently from accidents occurred in Three Mile Island (1979), Chernobyl (1986), and Fukushima Daiichi (2011) nuclear power plants. Since containment integrity in light water reactors (LWRs) is possible to be impaired, e.g., by hydrogen combustion in the early and intermediate stage of a severe accident, the uncontrolled release of FPs to the environment (“source term”) may occur. From Fukushima accident, it became clear that despite the combustible gas control inside the containment by the nitrogen inertization, the explosions outside the containment in the reactor building could not be prevented as there existed no mitigation measures for combustible gas control under severe accident conditions. The lessons learned from Fukushima accident underline the necessity to consider broader range of accident scenarios including external events with consequences not only on containment but also on spent fuel pool, and the surrounding reactor building [1].

In this context, a combination of safety as well as monitoring systems well qualified for the operation under a broad range of postulated severe accident scenarios are important to minimize the hazards associated with

Received Feb. 23, 2021; accepted Jul. 29, 2021; online Dec. 10, 2021

Sanjeev GUPTA (✉), Martin FREITAG, Gerhard POSS
Becker Technologies GmbH, Rahmannstrasse 11, Eschborn 65760, Germany
E-mail: gupta@becker-technologies.com

Special Issue: Innovative Nuclear Energy Technology

hydrogen (H_2) risk and the source term. To ensure that the installed safety or mitigation systems will operate as per their design capacity in the course of their application for severe accident management (SAM), it is of utmost importance to verify their effectiveness by means of experiments covering a wide range of accident scenarios, and by performing full-containment analyses by use of qualified safety analyses tools. As far as experimental research is concerned, consideration of realistic boundary conditions is necessary to assess active or passive safety systems for their effectiveness and risk balance considering both favorable and undesired effects under a wide range of postulated accident scenarios. This requires consideration of both the early as well as the late phase of an accident to incorporate variations as expected during the progression of an accident, such as containment thermal-hydraulics, physical and chemical properties of airborne FPs, varying gas composition e.g., O_2, H_2, CO, and CO_2 including conditions as expected during molten corium-concrete interaction (MCCI). Toward consideration of realistic boundary conditions, the specific experimental research needs for evaluating the impact of realistic severe accident conditions on FP behavior, e.g., effects of high temperature, dose rate, water impurities, energetic events such as hydrogen combustion on FP transport and distribution behavior in reactor coolant system (RCS) and/or containment, have also been underlined at the recently held committee on the safety of nuclear installations (CSNI)/ working group on analysis and management of accidents (WGAMA) international source term workshop [2].

International collaboration on research topics of safety relevance is becoming important to derive a commonly agreed approach for resolving the remaining open issues related to combustible gas risk and FP behavior including investigations related to safety and mitigation systems [3–6]. International collaborative experimental programs are highly beneficial since they enhance confidence in the performance of safety systems under a broad range of severe accident scenarios and help to establish a common database accessible by a large research community to support further development and validation of lumped parameter (LP) and computational fluid dynamics (CFD) codes.

The thermal-hydraulics, hydrogen, aerosols, and iodine (THAI) program provides contribution to these international co-operation activities, e.g., by providing data for validation and further improvement of severe accident modeling. The overall objective of the THAI experimental program is to investigate open issues related to the thermal-hydraulics, combustible gas behavior (e.g., H_2, CO), FPs (aerosol, iodine) transport and their interaction with containment structures and safety systems under realistic thermal hydraulic conditions. The experimental database produced in THAI or recently in the multiple-compartment ($THAI^+$) test facility is continuously used for the verification and validation of LP and CFD codes.

The present paper focuses on THAI/$THAI^+$ experiments, which investigated active or passive safety systems employed in LWR containments, e.g., suppression pool hydrodynamics, performance behavior of passive autocatalytic recombiner (PAR) and spray interaction with containment thermal-hydraulics and hydrogen-steam-air flames. The relevance of these experimental investigations for LP and CFD codes validation as well as for reactor safety application is highlighted with examples.

2 THAI program and test facility

The THAI experimental research program aims to provide containment specific experimental databases for validation and further development of LP- and CFD- codes used in the area of reactor safety analyses to investigate specific issues for LWR under severe accident conditions and to improve SAM measures: thermal hydraulics and water pool hydrodynamics; H_2/CO (combustible gases) distribution, combustion and recombination; and aerosols and iodine (FP) behavior.

The THAI experimental research is executed in the frame of national program sponsored by the German Federal Ministry for Economic Affairs and Energy (BMWi), and the international program run under the auspices of Organisation for Economic Co-operation and Development (OECD)/Nuclear Energy Agency (NEA). The main topics covered in the ongoing and concluded national and OECD/NEA THAI projects [7–20] are summarized in Table 1. Some of the topics, which have been investigated both in national and OECD/NEA THAI projects are conducted with different set of test parameters to provide complimentary database.

The experiments are conducted in the $THAI^+$ test facility, which is operated by Becker Technologies in close co-operation with Framatome, Erlangen, and GRS, Cologne. $THAI^+$ is an acronym for thermal-hydraulics, hydrogen, aerosols and iodine in multiple (+) compartments. The unique feature of the THAI/$THAI^+$ test facility is that experimental infrastructure and appropriate boundary conditions of the test facility make performing coupled-effect experiments possible by use of representative aerosol and combustible as mixtures, and thermal-hydraulic conditions. The spatio-temporal FP behavior can be studied by use of radiotracer I-123.

The $THAI^+$ test facility makes it possible to investigate various accident scenarios, ranging from turbulent free convection to stagnant stratified containment atmospheres and can be combined with simultaneous use of hydrogen, iodine and aerosol issues. The experimental configuration and the operating conditions in the test vessel can be established as typical of those for water cooled reactors (e.g., boiling water reactors (BWRs), pressurized water reactors (PWRs)) but the modular nature (e.g., removal internals), large top openings, and adequate design

Table 1 Overview of THAI experimental programs together with the investigated issues

Experimental program	Duration	Topics of investigation
National THAI-I [8,9]	1998–2003	Gas distribution in uniformly mixed or stratified gas atmosphere (including the effects of condensation, turbulence), I_2 distribution and interaction with steel surfaces
National THAI-II [10,11]	2003–2007	Gas distribution (blower jet), I_2 mass transfer, multi-compartment I_2 distribution and behavior, iodine interaction with painted surfaces, iodine-oxides distribution and behavior, dry resuspension of aerosol material by hydrogen deflagration (HD), wet aerosol resuspension from a boiling sump, PAR operation influence on iodine volatility
National THAI-III [12]	2006–2009	Stratified atmosphere dissolution by blower jet, natural convection in containment. I_2 gas/liquid mass transfer, I_2 interaction with painted surfaces
National THAI-IV [13]	2009–2013	Initially stable gas stratification and dissolution by natural or forced convective flows, I_2 deposition and washdown behavior from condensing painted surfaces, aerosol (soluble/insoluble mixture) washdown from surfaces, soluble/insoluble aerosol resuspension from a boiling sump, BWR pressure suppression pool hydrodynamics (thermal stratification, bubble dynamics, pool swelling)
National THAI-V [14]	2013–2017	Stratified flows in containment-constant pressure, water hydrodynamics (WH)-incomplete condensation, I_2 multicompartment tests including influence of paint/aerosol/relative humidity, airborne aerosol and iodine wash off by spray, I_2/Ag reaction in the sump, PAR performance under counter-current flow conditions
National THAI-VI/VI-b [15,16]	2017–2021	Aerosol pool scrubbing, multi-compartment HD, I_2 distribution in room chain, PAR performance/ignition behavior in H_2/CO containment atmosphere
National THAI-VII	2021–2023	Counter-current flow in multicompartment geometry, heat transfer by free convection at large Rayleigh numbers (small modular reactor oriented), degradation of the painted surfaces in containment by HD
OECD/NEA THAI [17]	2007–2009	Gas distribution (stratification, condensation), PAR performance under conditions (start-up, ignition, and performance under oxygen starvation conditions (SA)), H_2 deflagration, interaction between gaseous iodine and airborne aerosols (SnO_2 and Ag), aerosol (soluble) washdown from surfaces
OECD/NEA THAI-2 [18]	2011–2014	PAR performance- start-up and ignition behavior in reduced O_2 conditions, H_2 combustion-spray interaction, release of gaseous iodine from a flashing jet (PWR design basis accident (DBA) scenario)
OECD/NEA THAI-3 [19]	2016–2019	PAR performance under counter-current flow conditions, multi-compartment H_2 deflagration with initial natural convection, aerosol and iodine re-entrainment from water pool incl. The effect of surfactants on aerosol re-entrainment behavior, aerosol and iodine resuspension from surfaces by HD including thermal decomposition of CsI aerosols to gaseous I_2
OECD/NEA THEMIS [20]	2020–2024	PAR performance under H_2-CO and iodine-oxide aerosols containing atmosphere, H_2-deflagration behavior under H_2-CO-CO_2-steam containing atmosphere, pool scrubbing under jet regime, iodine-oxide and nuclear aerosols interaction in containment atmosphere

boundary conditions of the test facility also allow diverse experimental investigations including performance testing of passive safety systems.

The original single-vessel THAI test facility has been in operation since 2001 and was designed and constructed based on the experience gained with the battelle model containment (BMC) test facility (Fig. 1), which had also been operated with involvement of Becker Technologies personal. The THAI facility allowed to continue the investigations performed at BMC but under broader and well-controlled boundary conditions (e.g., controlled vessel wall temperature, elevated pressure, radio-tracer I-123 for online, and long-term iodine measurement). In 2015, the original THAI facility was extended to THAI$^+$ configuration by adding a second vessel named parallel attachable drum (PAD) in a tow-vessel configuration (Fig. 1). The extended THAI$^+$ test facility broadens the experimental capability and allows to generate a wide range of complex scenario-specific conditions, e.g., by establishing inhomogeneous atmospheric conditions, natural convection flow loops, counter-current flows, or multi-compartment conditions.

The THAI$^+$ configuration with main dimensions is shown in Fig. 2. The main components of the THAI$^+$ facility are two cylindrical steel vessels connected by DN 500 pipes at the top and the bottom, the THAI Test Vessel (TTV) is 60 m^3, 9.2 m high, and 3.2 m in diameter and the PAD vessel is 17.7 m^3, 9.73 m in height, and 1.6 m in diameter, with a sump compartment at the lower end of each vessel (Fig. 2). The vessel and pipes are fully insulated by mineral wool enveloped with aluminum cladding. The wall temperatures of both vessels can be controlled through an external thermo-oil circuit. The THAI$^+$ test facility has the same design boundary conditions as those in the original THAI test facility (1.4 $\times$ 10^6 Pa at 180°C) and retains its unique experimental features, e.g., use of hydrogen and iodine tracer I-123, and differential wall heating/cooling.

As per the experimental requirement, it is possible to perform experiments in a single-vessel configuration alone (TTV or PAD) or in the THAI$^+$ two-room vessel geometry. In addition to lower manhole, top openings (THAI: 1.54 m, PAD: 1.4 m in diameter) provide access to the vessel for installing instrumentation or test specific hardware. The

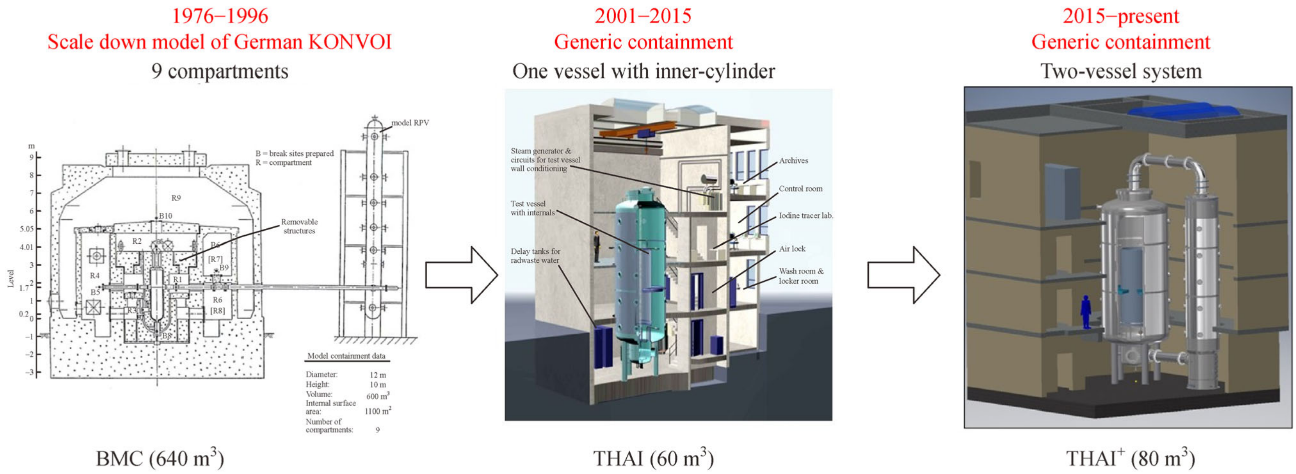

Fig. 1 Test facilities: BMC, THAI, and THAI$^+$.

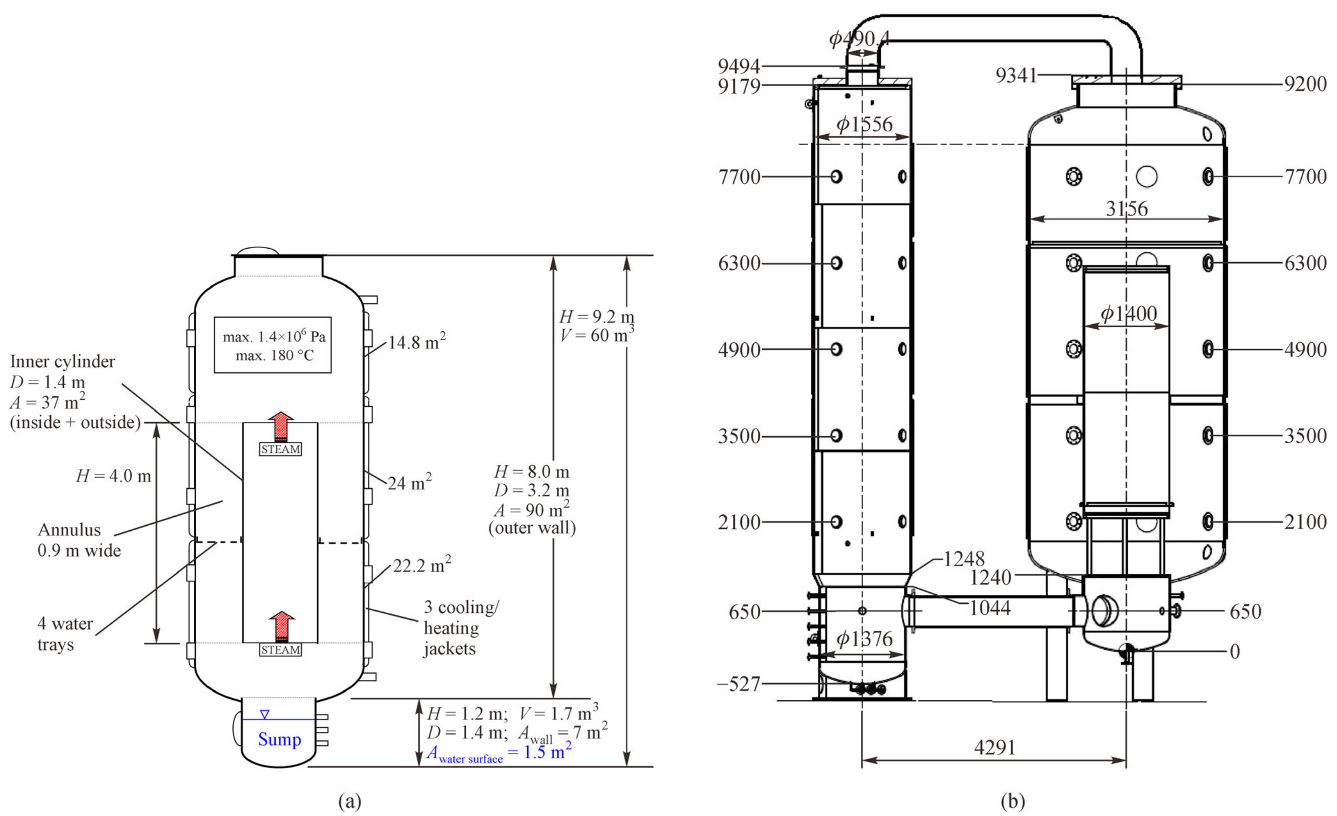

Fig. 2 Configuration and dimension.
(a) THAI; (b) THAI$^+$.

modular nature of the test facility for investigating a broad range of topics is demonstrated in Fig. 3 with selected test configurations of the THAI/THAI$^+$ test facility.

Large efforts have been made to monitor local and large-scale flows inside the test facility by field measurements in the bulk as: laser-doppler anemometer (LDA) for 2-D velocity and turbulence measurements, 2-D and 3-D particle image velocimetry (PIV) with a field-of-view of up to 2 m^2. The volumetric flow being exchanged between the two vessels (TTV and PAD) can be measured using a unique measurement device (METUSA). It consists of two rotatable flanges which envelope an 885 mm long DN 500 pipe-section equiped with 6 vane wheels to scan flow profile in the entire pipe cross section. For iodine

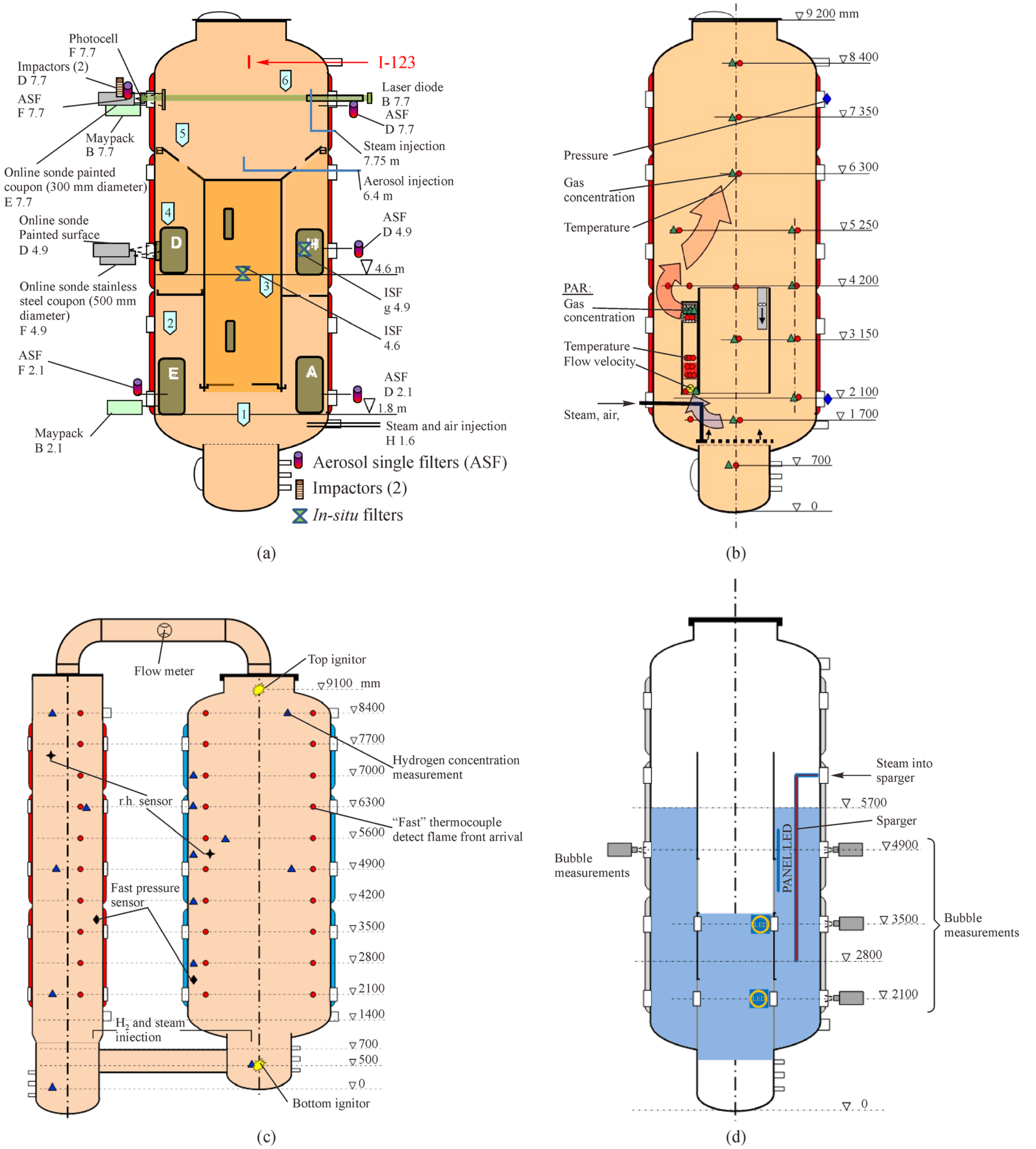

Fig. 3 Examples of THAI/THAI$^+$ test configurations.
(a) Iodine multi-compartment test; (b) PAR performance tests; (c) H_2 deflagration (multi-compartment) behavior; (d) water pool hydrodynamics.

distribution measurements, radioactive iodine I-123 is used as a tracer for inactive iodine, and liquid and gas samples are taken at numerous locations. The iodine concentration in the gaseous phase is determined by gamma-ray evaluation of samples from *in situ* gas scrubbers, or from Maypack filters, the latter discriminating molecular, organic, and aerosol-borne iodine. A wide spectral light absorption spectroscopy called light absorption system for I_2 using spectroscopy (LASI-SPEC), which provides a continuous, in-line, and non-intrusive measurement of gas borne iodine is available for measurements in both vessels. The details of the available instrumentation and measurement techniques in the THAI/THAI$^+$ test facility including the details of measurement accuracy are provided in Refs. [21–23].

The THAI experimental database contributes to the validation and further development of advanced LP codes (e.g., AC^2/Containment Code System (COCOSYS), ASTEC, and MELCOR) and CFD codes (e.g., CFX, FLUENT, GOTHIC, GASFLOW, FLACS, and OPEN-FOAM) used by the THAI project partners, e.g., by providing experimental data for code benchmark exercises. A selection of code benchmarks and joint analytical activities based on the THAI/THAI$^+$ test data are summarized in Table 2.

THAI experimental data have demonstrated a reliable simulation of complex experiments, e.g., hydrogen distribution (OECD-THAI HM-2 code benchmark), PAR performance (OECD-THAI-2 HR-35 code benchmark), and hydrogen combustion behavior (ISP-49), etc.

The application of LP and CFD codes for THAI deflagration tests provided useful insights. The OECD/

Table 2 Application of THAI/THAI$^+$ experiments for code benchmark exercises

Project/Frame	Issue	THAI experiment
Containment thermal-hydraulics, hydrogen distribution		
OECD/NEA THAI	Hydrogen distribution, stratified flows in containment	Erosion of stable atmospheric stratification layer by a buoyant plume: based on test HM-2 using H_2 [24]
OECD/NEA ISP-47	Hydrogen distribution, containment thermal hydraulics	Based on THAI test TH-13 [25]
German CFD network	Gas distribution, thermal-hydraulics	THAI thermal hydraulics separate- and coupled-effects experiments for CFD and LP code benchmarks, e.g., - international code benchmark based on THAI test TH-24 [26] - international code benchmark based on THAI test TH-27 [27] - international code benchmark based on THAI test TH-32
Hydrogen mitigation-PARs		
OECD/NEA THAI 3 [19]	PAR operation under counter current flow conditions	Based on test Hydrogen Recombiner (HR)-49
OECD/NEA THAI 2 [18]	PAR performance in gas atmosphere containing low O_2 concentration	Based on test HR-35
OECD/NEA THAI [17]	PAR performance under accident conditions	HR test series, validation and further development of PAR specific models/ empirical correlations, PAR ignition models, code validation and application to reactor situations [28]
EC/Severe accident research network of excellence (SARNET2), WP7	PAR performance behavior	Benchmark on THAI tests PAR-2 and PAR-4
Hydrogen combustion		
OECD/NEA THAI-3 [19]	HD with initial natural-convection flow conditions	Based on test HD-44
OECD/NEA THAI-2 [18]	HD under spray	HD 31 – 35 test series
OECD/NEA THAI [17]	HD in premixed gas atmosphere (upward/downward burn)	HD 1 – 30 test series
OECD/NEA ISP-49	Hydrogen combustion	Based on THAI HD tests HD-2R (open) and HD-22 (blind), and French test facility non-uniformity of hydrogen concentration the fast combustion regime (ENACCEF) [29]
FP (Aerosols, Iodine)		
OECD/NEA THAI-2 [18]	Interaction of molecular iodine and aerosols in containment atmosphere	THAI tests Iod-25 (SnO_2-aerosol) and Iod-26 (Ag-aerosol)
EC/SARNET (Phase 1), WP1	Iodine mass transfer	Joint interpretation of THAI Iod-9 and code benchmark [30]
EC/SARNET (Phase 2), WP8	Iodine oxide behavior	Joint interpretation of THAI tests Iod-13 and Iod-14 [31]
EC/SARNET (Phase 2), WP8	Multi-compartment Iodine behavior	Code benchmark on THAI tests Iod-11 and Iod-12 [32]

NEA THAI-2 [18] project deflagration tests in the presence of operating spray system covered a broad range of accident typical conditions by parameter variations. The data proves clearly that the interaction between airborne water droplets and flame deflagrations need to be considered in code models and for new safety analyses, since it affects not only the pressure and temperature load on the containment, but also the propagation of flames. Several organizations had already started to incorporate these results into their code models in order to improve prediction of flame dynamics and pressure response. Both LP and CFD codes indicated difficulty in reproducing turbulence enhancing effect by spray to correctly simulate spray and combustion interaction. Indeed, the role of water sprays on premixed flame propagation is complex and depends strongly on several parameters such as the airborne liquid water fraction (a function of spray water mass flow and the mean droplet falling velocity), droplets distribution inside the containment atmosphere and droplet size.

In the case of PAR investigations, a deep insight into their performance and ignition potential under accident typical conditions has been obtained based on THAI/THAI+ experiments. An overview of analytical activities based on THAI PAR tests is provided in Ref. [28].

The THAI experiments on FP behavior cover a wide spectrum of accident scenarios and provide relevant data for validation and development of iodine and aerosol models implemented in the severe accident analysis codes, e.g., AC²/COCOSYS [33–36]. Based on THAI test Iod-29 [18] which investigated the I_2 release from flashing jet, the lack of validation of existing iodine chemical models in the aqueous phase for reactor coolant circuit conditions relevant for PWR DBA was also identified. Recently, the OECD/NEA THAI-3 [19] project data on FP release from boiling pools and on FP remobilization from surfaces due to hydrogen combustion have offered a unique database to assess in-containment airborne radioactivity during a severe accident. The experimental results from these tests have been used to assess the source term in severe accident code calculations of the Fukushima-Daiichi accident in the assessment of continued releases in the days following the accident.

3 Main outcomes from THAI experimental research

3.1 Containment spray

The main focus of the spray tests conducted in the THAI/THAI+ test facility was to provide phenomenological insights on the remaining open issues together with suitable database to support validation and further development of spray-modeling capabilities of the existing safety analysis codes [37,38]. The spray tests conducted in THAI or THAI+ configurations include the effect of spray operation on containment thermal-hydraulics (pressure/temperature), the spray induced pool mixing in wetwell, the spray interaction with hydrogen combustion flames, and the effect of spray on FP (aerosols, gaseous iodine) washout from containment atmosphere.

Different test configurations used for the above-mentioned spray tests are depicted in Fig. 4. For the tests of Aerosol Washdown (AW)-4, Iod-31, and HD 30–35 discussed in this section, a full cone whirl spray nozzle (BETE, model No. 3/4 WL1230) was used. The injected water mass flow rate was 1 kg/s. The spray characteristics like gas volume per spray nozzle, spray water flow rate per nozzle, droplet size distribution, are in close proximity to the spray systems installed e.g., in French PWR, Korean Advanced Power Reactor (APR) 1000, or Russian Water-Water Energetic Reactor (VVER)-440/213 nuclear power plants (NPPs). A spray angle of 30° was chosen to exclude the spray interaction with THAI vessel walls, which might otherwise influence system pressure progression due to droplet evaporation on heated walls. The spray nozzle installation position in the test of Iod-31 was in an optimized position to minimize wall wetting and facilitate homogeneous iodine distribution between two interconnecting vessels due to mixing by gas entrainment. For the test of TH-19 and tests series of WH 1–6, spray characteristics are oriented toward the spray system installed in German BWRs.

3.1.1 Effect of spray on containment thermal-hydraulics

The effect of spray operation on evolution of containment atmosphere temperature and pressure was studied in test Thermal-Hydraulic (TH)-19 by using a spray design similar to the one installed in the wetwell of German BWR type-69 design using a spray-nozzle type Lechler 120° axial full cone (Model Nr. 461.048.17.AK.00.0). The spray nozzle used for testing had a nozzle inlet diameter of 7.6 mm and a water flow rate of 0.8 L/s. The spray produced droplets with a sauter mean diameter (SMD) of 0.75 mm. The initial absolute pressure was 0.2 MPa. The results reveal that after reaching a certain falling distance, a thermal equilibrium is reached between spray droplets and the surrounding gas atmosphere. The cooling efficiency increases with increasing drop height and decreasing droplet size. The transient heating of the droplets as a function of the falling distance can be described as a first approach by Eq. (1) [39].

$$T(z) = T_{\mathrm{atm}} - (T_{\mathrm{atm}} - T_0)\ \exp(-z/w), \tag{1}$$

with $T(z)$ being the droplet temperature after falling distance z; T_{atm}, the temperature of the vessel atmosphere; and T_0, the initial droplet temperature. The parameter w describes the overall heat transfer between atmosphere and droplets including the heat of condensation. The parameter

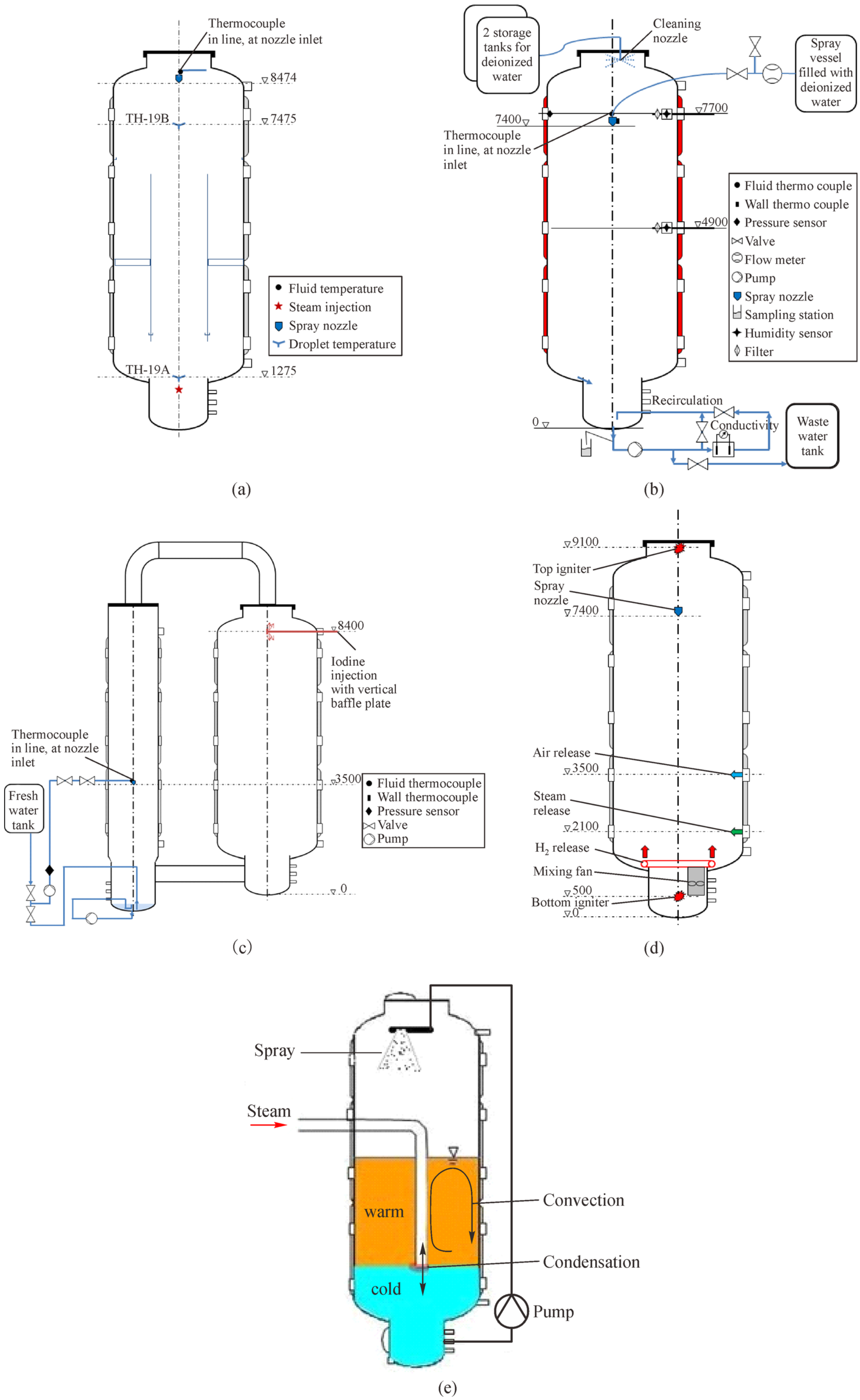

Fig. 4 Test configurations for spray tests in THAI/THAI^{+} test facility.
(a) Gas mixing test series TH-19; (b) aerosol washout behavior (Test AW-4); (c) iodine washout behavior (Test Iod-31); (d) spray interaction with H_2 deflagration (Tests HD 30–35); (e) thermally stratified water pool mixing by spray (Tests WH 1–6).

w is determined based on measured experimental values which can be described by Eq. (2) [39].

$$w = w_0 \left(\frac{T_{\text{atm}} + T_0}{T_{\text{atm}} - T_0} \right)^4, \tag{2}$$

with constant w_0 determined to be 0.083 m for the THAI spray-nozzle.

On the subject of spray induced condensation affecting the combustible gas concentrations, test HD-31-SE was conducted in THAI. The test objective was to investigate the spray induced steam condensation behavior in containment gas atmosphere, which increased the volumetric concentration of the combustible non-condensable gases with the threat of a more severe combustion. The spray nozzle with a 30° spray angle was installed at the centerline of the vessel at the elevation of 7.4 m. The test was conducted at a pressure of 0.15 MPa, a gas temperature of 90°C, and a volume fraction of 25% steam in air. The spray water temperature and SMD of the water droplets was 20°C and 600 μm, respectively. The vessel atmosphere could be divided into three parts as per the observed spray effect, i.e., vessel atmosphere above the spray nozzle: this part of the vessel shows slow steady temperature decrease indicating lack of immediate mixing of the H_2 containing gas mixture; vessel atmosphere below the spray nozzle, but outside the spray cone: this part of the vessel shows faster and steady decrease indicating an efficient mixing of the gas atmosphere; and within the spray cone: fast decrease within the first 10 s after start of spray, thereafter steady decrease.

The evolution of gas temperature due to an operating cold-water spray is shown in Fig. 5. The pressure change during this phase is mainly governed by the temperature decrease of the gas phase (resulting into pressure decrease), the condensation of steam (resulting into pressure decrease), and the partial vaporization of droplets (resulting into pressure increase).

The test results indicate that the effect of spray on steam condensation is not an instantaneous but a gradual process. In the long term, pressure and gas temperatures decrease as long as the spray is active. The steam condensation due to the cold-water injection is only partially compensated by vaporization of spray droplets. Since most of the heat transferred to the droplets is used for heating the droplet water body from 25°C to surrounding gas temperature, only a very small amount of water might vaporize. For the investigated test conditions with homogeneously mixed gas atmosphere, the depressurization rate and temperature decrease rates were in the order of 220 Pa/s and 0.1°C/s, respectively.

3.1.2 Effect of spray on H_2 combustion behavior

The data for an improved understanding of hydrogen combustion phenomena in combination with the use of spray systems are obtained from the tests conducted in the frame of the OECD/NEA THAI-2 project [18]. The tests were conducted with systematic variation of the test parameters, e.g., initial gas temperature, steam content, spray water temperature, spray droplet size, spray duration before ignition, and burn direction. The resulting influence on pressure build-up, temperature development, flame front propagation, and completeness of combustion was quantified. Both spray water and initial gas temperatures were varied to investigate spray induced condensation/ evaporation effects by operating cold water spray in hot

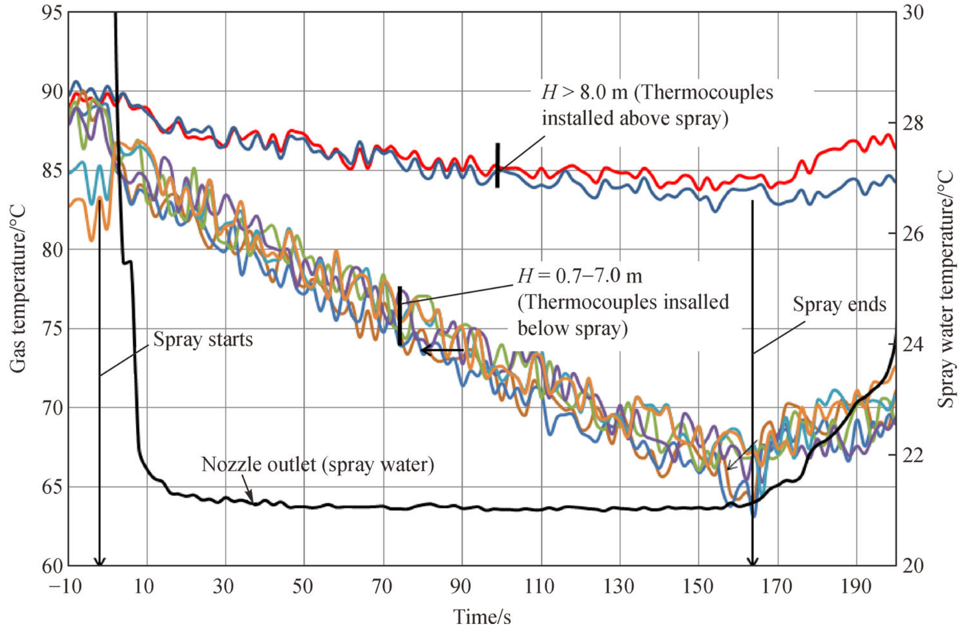

Fig. 5 Effect of spray operation on temperatures in vessel gas atmosphere.

gas atmosphere or hot water spray in hot gas atmosphere, respectively. For studying the mixing effect, two different nozzles with spray droplets SMD of 670 μm or 970 μm were used.

In addition to condensation, the turbulence generated by spray operation is also of interest to quantify the overall effect of spray operation on hydrogen combustion behavior. In quiescent atmosphere, expanding gases produce some turbulence in the unburned mixture, which, in turn increases the flame front velocity. In case of upward burn direction, turbulence generation is supported by the buoyancy effect due to the large temperature difference (i.e., density difference between the hot already burnt gas and the surrounding cold unburned gas), which can develop to large scale turbulence in the course of combustion. In case of downward burn direction, some small-scale turbulence is produced. The presence of a mixing fan or internal structures in a closed atmosphere may further enhance the turbulence effect on flame propagation behavior, e.g., flame propagation without satisfying the minimum hydrogen threshold needed for flame propagation to occur in a specific direction [40].

For the THAI tests without spray in pre-mixed, quiescent atmosphere, the hydrogen concentration threshold for downward burn direction was determined to be 8.7% H_2 (volume fraction) in air at ambient temperature and initial vessel pressure of 0.15×10^6 Pa. In case of a gas atmosphere temperature of 90°C and with a steam concentration of volume fraction of 47% (saturation state) being determined to be 12% hydrogen (volume fraction), downward burn (Fig. 6(b)) (i.e., hydrogen concentration > 8.7% (volume fraction)) always resulted in complete combustion in all tests, which was indeed not the case always for upward burn at least for ⩽7.5% hydrogen concentration (volume fraction) [17]. A pronounced flame acceleration starting at a very low speed was observed in case of downward burn.

As far as the application of experimental findings (without spray) on peak pressure and peak temperature is concerned, particularly for slow HDs with rather long combustion times, the heat transfer to surfaces driven by gas-surface temperature difference is one of the important parameters, which shall be taken into account while transferring experimental results to the reactor scale. As shown in Fig. 7, THAI combustion tests exhibit markedly low values for peak pressure and peak temperature as compared to the corresponding adiabatic-isochoric-complete-combustion (AICC) values. In the investigated test cases, the slow combustion lasts for several seconds, which allows a substantial heat transfer to structures, and additionally, in some of the tests, the combustion is incomplete.

For the THAI HD tests with spray, for which a nozzle with the same droplet size distribution as for the NPP was used, i.e., a droplet size of 670 μm (SMD) and a water mass flow rate per nozzle of 1 kg/s, confirm the advantageous effect of spray operation with these nozzles with respect to deflagration peak pressure reduction for most of the investigated test conditions. For the flame quenching process approaching to complete flame extinction, the total available droplet surface was determined by a decisive parameter. This is a function of the airborne water concentration (a function of spray water mass flow and the mean droplet falling velocity) and the droplet size distribution.

The comparison between tests with different burn directions (upward and downward) revealed that all spray tests with a H_2 concentration of up to 10% (volume fraction) and upward combustion exhibits clearly a suppressing effect with respect to peak pressures and peak temperatures which becomes more pronounced for higher steam contents. The only test with a higher peak pressure compared to reference test without spray was the test HD-35 conducted with a H_2 concentration of 12% and 25% (volume fraction) steam and downward burn direction, for which the peak pressure exceeded that of the

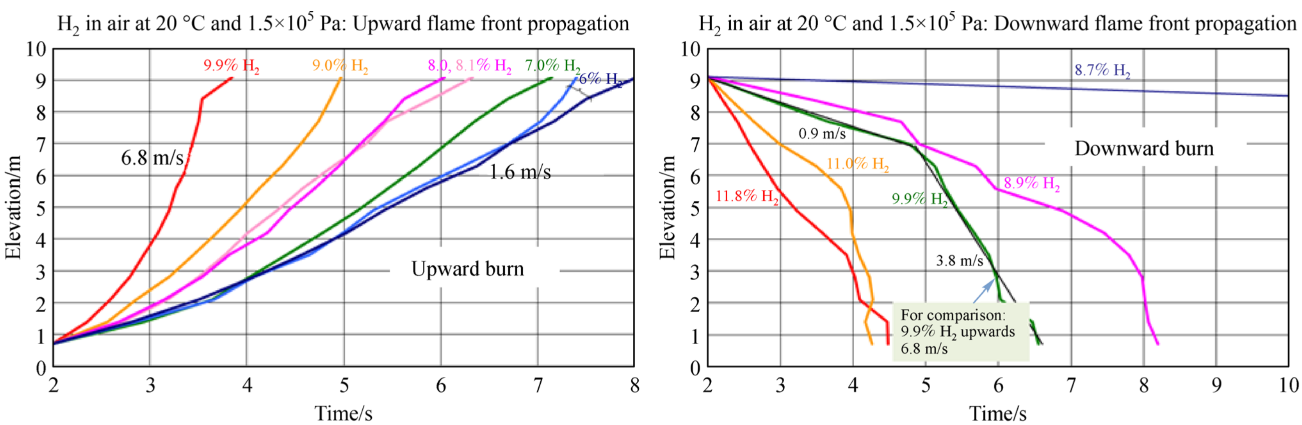

(a) (b)

Fig. 6 Flame front propagation as a function of H_2 concentration in THAI tests without spray.
(a) Upward burn; (b) downward burn.

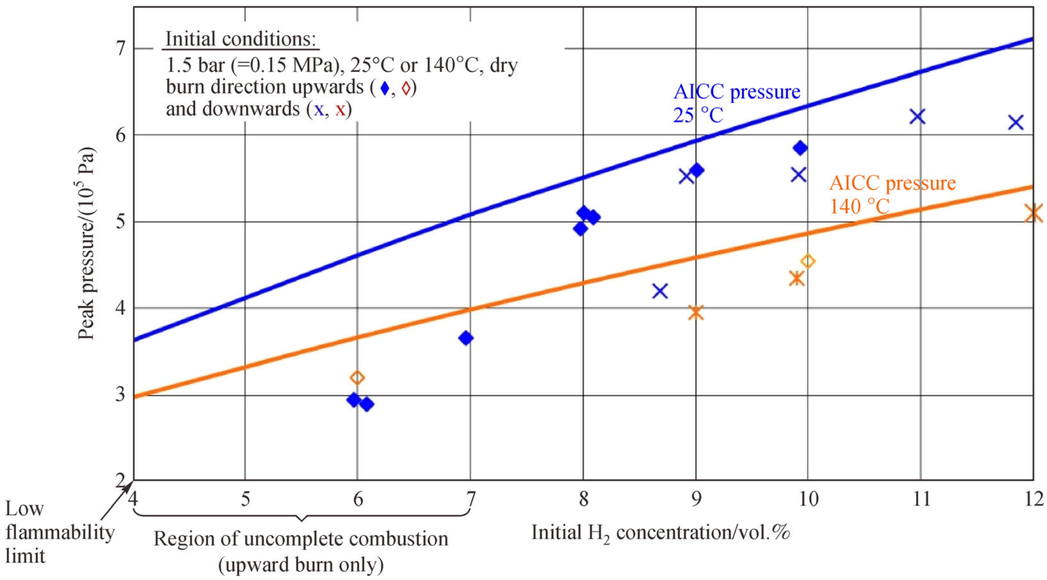

Fig. 7 Comparison of peak pressure and peak temperature to AICC data in THAI tests (without spray) with upwards and downward burns.

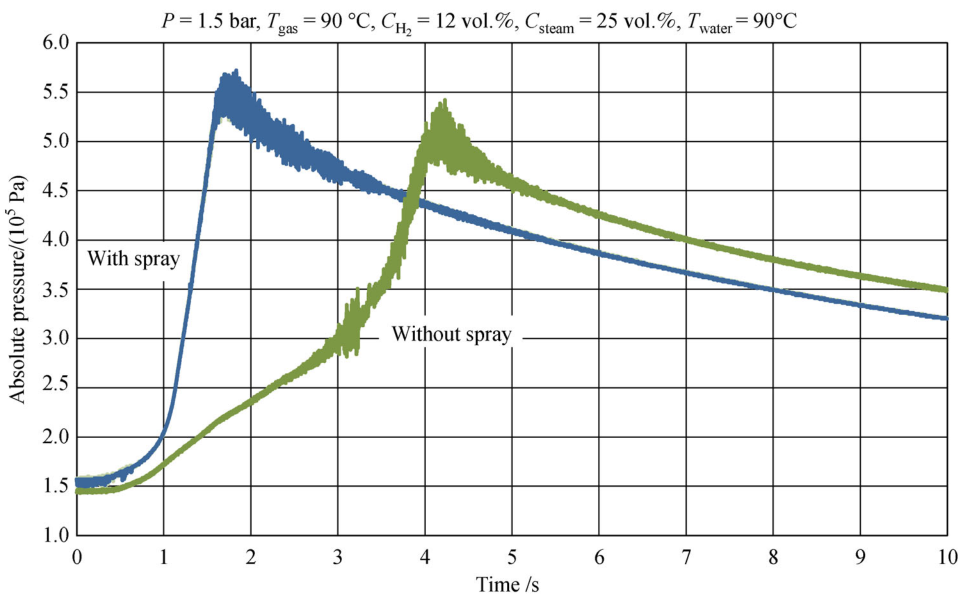

Fig. 8 Effect of spray on vessel pressure evolution in downward combustion case.

quiescent (without spray) test HD-23 by 10%. As shown in Fig. 8, the test results show an increased pressure peak (about 10%) during spray operation as compared to the test without spray. The pressure data have been normalized with P_{max} that corresponds to the maximum measured pressure in test HD-35.

However, it should be noted that a gas mixture with a H_2 concentration of 12% (volume fraction) is strongly sensitive for flame acceleration in a turbulent flow field. Since this sensitivity increases exponentially with the H_2 concentration (Fig. 6), a mixture with a H_2 concentration of 10% (volume fraction) would be less sensitive to flame acceleration. Therefore, the difference between a test with and without spray with respect to peak pressure and peak temperature should be much smaller for such a mixture as compared to the cases with a higher H_2 concentration in the containment atmosphere.

Regarding the flame propagation behavior, the tests with downward burn revealed that the flame speed above the spray nozzle is the same as for the reference test without spray. However, after having passed the nozzle location, the flame speed becomes extremely high due to the superimposition of the downward directed flow produced by the gas entrainment of the spray. In addition to the downward directed flow, the spray droplets induce turbulent fluctuations which promote flame acceleration.

Transferring the THAI experimental outcomes to the reactor case, it was shown that by use of the cold-water spray in a saturated atmosphere, steam condensation takes place over a long duration of its operation and may render non-flammable mixtures flammable. The combustion near the flammability limit is benign with very moderate pressure increase for low and intermediate H_2 concentrations. Early spray activation may be considered favorable, since for an accident scenario with a H_2 concentration exceeding 8% (volume fraction) (in ignitable atmosphere) despite PAR operation, several sources of ignition are present in a containment building, e.g., random ignition (TMI, non-nuclear industry experience), by an operating PAR, or by glow plugs. For this case (H_2 concentration in the range of 8% (volume fraction)), the flame suppressing effect, i.e., peak pressure reduction, of the spray is considered beneficial.

3.1.3 Etffect of spray system on mixing of water pools

The pressure suppression pool in a BWR prevents containment pressure build-up during a loss-of-coolant accident (LOCA). In case of a LOCA, after the blow down has taken place, weak mixing in the pool due to a low mass flow rate of steam (without non-condensation gas fraction) can cause a thermal stratification in the pool and thus, reduce the pressure suppression capacity. The THAI experiments were conducted with an aim to provide a necessary database on the spray induced water pool mixing and cool down behavior.

To carry out these experiments, the THAI vessel was filled with water up to the elevation of 5.2 m, representing a water pool volume of 29 m^3. The varied parameters included steam mass-flux ($\dot{m}_s$ = 0.94–2.35 kg/(m^2·s), submergence depth (2 m), initial water pool temperature (T_w: 10°C–60°C), and vessel pressure (0.1 × 10^6–0.2 × 10^6 Pa). A test was conducted with reduced water inventory (1/4 reduction) and reduced submergence depth (0.5 m).

After preparation of the initial test conditions, the experiments were performed with two phases. In the first phase, steam was injected at the desired mass flow rate until the stratification developed and the target maximum water temperature difference of about 25°C between the

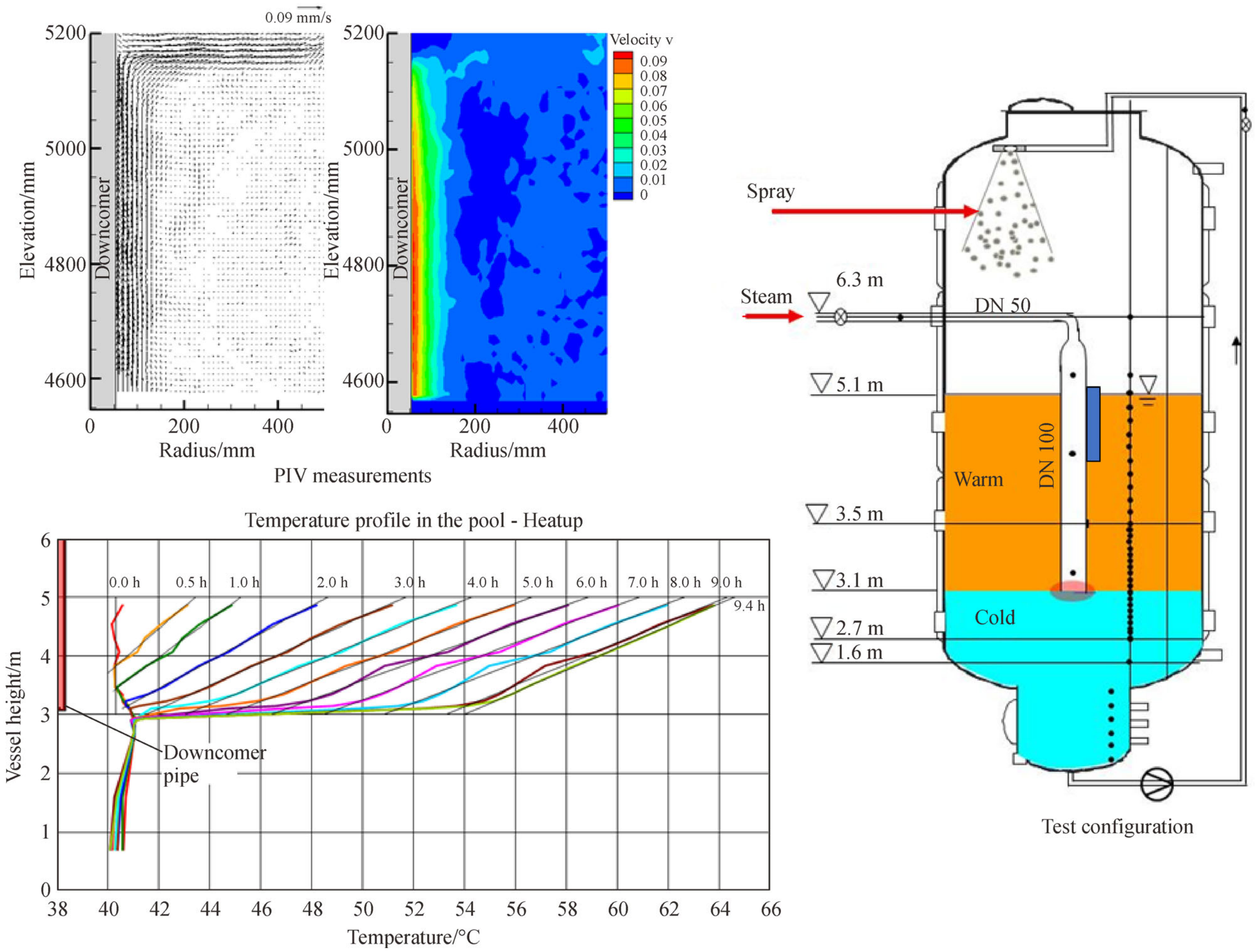

Fig. 9 Field measurements with PIV, and temperature profiles measured with thermocouples in the pool during the heat-up phase for T_w = 40°C and $\dot{m}_s$ = 2.35 kg/(m^2·s).

lowermost and uppermost water layer was achieved. In the second phase, stratification break-up by means of a water spray and resulting water pool mixing behavior was investigated. A loop was installed to recirculate pool water from the bottom part of the THAI vessel and sprayed back on the pool surface by a 15 mm diameter hole (Fig. 4(e)). The cooling phase was continued until a uniform temperature in the water pool had been achieved.

Figure 9 shows the development of thermal stratification along the water pool elevation over a time span of 9 h. Time t = 0 h corresponds to the initiation of steam injection. With the start of steam injection, as shown in PIV measurements, a buoyant boundary layer develops over the length of the outer surface of the downcomer due to the heat conduction through the pipe wall. The stratification process starts almost immediately above the downcomer outlet after the steam injection begins. Due to buoyancy, all steam exiting from the downcomer pipe tends to turn upwards and there is no measurable change in temperature below the downcomer exit during the steam injection phase, thus showing a poor thermal exchange with the water body located below downcomer pipe for the investigated low steam mass-flux release case.

The water pool heat-up rate was determined based on the water temperature measured with a thermocouple array (Fig. 9). The heating-up rates were higher at higher elevations due to the occurrence of maximum heat input by the rising warm water in the boundary layer formed along the downcomer pipe wall, where PIV measurements also showed higher velocities as compared to the surrounding fluid (Fig. 9). Figure 10 depicts an example of the pool heat-up rate as a function of water pool elevation. The heat-up rates are higher for higher elevations, where the

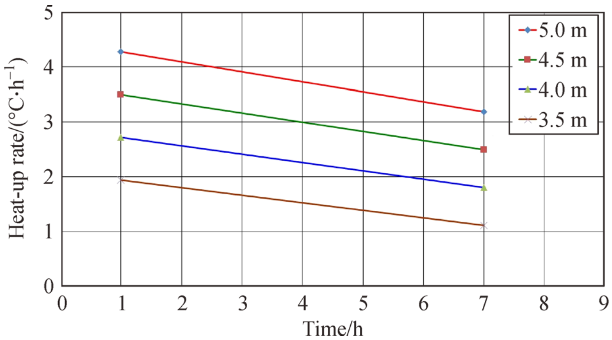

Fig. 10 Water pool heat-up rate at different pool elevations, for T_w = 10°C, $\dot{m}_s$ = 2.3 kg/m^{2}s.

heat transfer is higher, and decrease by time. The latter is a consequence of the decreasing temperature difference between injected steam and pool as the pool water is heated-up.

The second test phase started with initiation of the water spray (Fig. 11). The water was recirculated at a constant volumetric flow rate of 12 Nm^3/h and injected into the gas space. Recirculated spray provides an effective means to quickly mix the thermally stratified water pool and the cooling rate increases with a decrease in the initial water pool temperature (Fig. 11). The comparison of tests with different initial pressure indicates a more rapid cooling-down for the test with the higher initial pressure. The test with reduced initial water inventory (pool height 3.6 m instead of 5.1 m and downcomer submergence of 0.5 m instead of 2.0 m), exhibits the most rapid dimensionless temperature decrease, which is plausible, since the water flow rate (12 m^3/h) is the same as for the other tests, but the

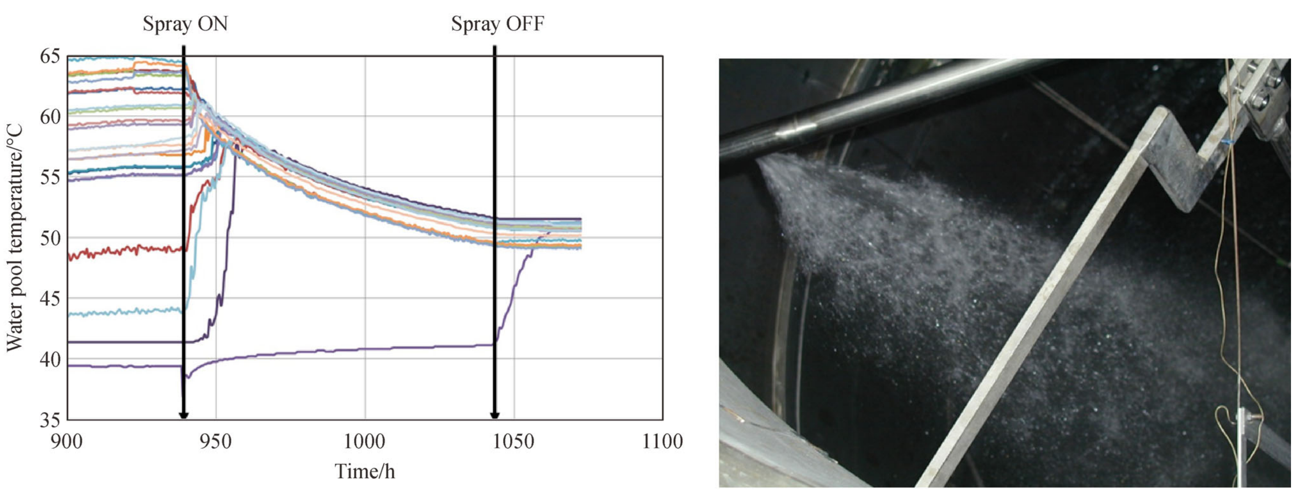

Temperature distribution along the pool height

(a)

Spray injection (vessel atmosphere)

(b)

Fig. 11 Water-pool thermal stratification and spray induced mixing.
(a) Temperature decrease and mixing in water pool; (b) after starting the spray operation in recirculation mode.

pool water inventory to be cooled down is reduced to 1/4 of water pool volume in other tests.

3.1.4 Effect of spray operation on FPs (aerosols and gaseous iodine) washout behavior

In addition to maintaining containment integrity by limiting containment pressure and temperature, spray operation plays an important role in reducing the gasborne inventory of radioactive material (aerosols, iodine) by washing them out from containment gas atmosphere. The sprayed water is generally collected in a sump at the containment bottom and can be recirculated for long-term spray operation. The modified conditions (e.g., temperature, pH, additives) in recirculated sump water, which may differ depending on the reactor design and the prevailing conditions following an accident, need to be considered for (recirculated) spray performance testing under accident conditions.

THAI/THAI$^+$ tests on the effect of spray operation on FP washout studied CsI-aerosols and molecular iodine (I_2). For aerosol test (AW-4), about 200 g of CsI was injected into the 60 m^3 THAI vessel. In case of iodine washout test, approximately 1 g iodine labeled with I-123 radiotracer was injected into the THAI vessel, and the spray was installed in the PAD vessel.

The efficiency of CsI-aerosol removal by spray has been determined by direct comparison of aerosol depletion in the tests conducted under the same conditions but either without or with spray operation. Accordingly, the test procedure consisted of two parts. In the first part (part A), the deposition behavior of CsI by sedimentation without spray has been monitored. After cleaning the vessel, the second part of the test (part B) was started by injecting CsI aerosol again into the vessel. Then, the wash-out of aerosol has been investigated by spraying water into the vessel twice, lasting 40 s each time. The aerosol size distribution and airborne aerosol concentration are measured before and after the spray operation. Time $t_A = t_B = 0$ min corresponds to the start of CsI aerosol injection in parts A and B. The results reveal that a spray system is efficient in removing aerosol particles larger than 1.0 μm in size (mass median diameter (MMD)). However, once the aerosol concentration is reduced and only very fine aerosol particles remain airborne, spray induced aerosol wash-out becomes less effective. The application of experimental results to reactor conditions imply that aerosol particles of intermediate size classes, between 0.1 μm and 1 μm are unlikely to be captured by falling spray droplets and will, therefore, remain airborne also during much longer spray operation. Future investigations are necessary in order to evaluate the effect of higher steam concentrations resulting into larger diffusiophoresis and increased hygroscopicity of the aerosol material.

In case of iodine washout test (Iod-31), the amount removed by spray was approximately 25% of the initially injected molecular iodine amount. The decrease in gas phase iodine inventory resulted in iodine increase in the sump water, into which the spray droplets are collected, with an equal amount. The efficiency of a spray system for wash-out of gas borne molecular iodine was found to be maximum when the gas atmosphere was sprayed with alkaline water (pH = 11) as compared to acidic water spray at pH = 4.5 or recirculated sprays with loaded iodine from the sump. In addition to useful insights on the spray effect on iodine washout from containment atmosphere, valuable data for the development and validation of the I_2 spray model, e.g., in COCOSYS/Advanced Iodine Model (AIM) were obtained. For transferring Iod-31 results to reactor scale, differences between test configuration and containment should be taken into account, such as gas-volume covered by the spray cone, spray droplets falling height, radiation effect, and available deposition surfaces for I_2 reaction.

3.2 PARs

PARs have become one of the primary measures to mitigate the combustible gas risk for severe accidents in current and advanced water-cooled NPPs. Post-Fukushima accident, there has been enhanced focus to consider PARs for combustible gas control considering numerous benefits associated with their passive nature and capability to start mitigating H_2 risk far below the lower flammability limit of H_2. As a result, many NPPs worldwide have either installed or being in the process of installing PARs inside the containment [1]. Even though post analyses of Fukushima accident did not have any major impact on existing PAR designs, it clearly emphasized the need of PAR performance testing, particularly the impact of late-phase accident conditions, e.g., O_2-lean, CO/CO_2 presence, high steam concentration, as the data are very sparse specially for the purpose of validation and further improvement of PAR-specific modeling. The need for complete and reliable data on PAR performance under severe accident conditions is indispensable for both supporting PAR implementation in containments and simulations of accident scenarios using computer codes based on different modeling approaches, e.g., LP, CFD, and mechanistic codes.

Investigations on PARs have been an important part of THAI experimental research and more than 50 PAR specific tests have been conducted in the framework of national and OECD/NEA THAI projects (Table 1). The main topics of PAR investigations already covered in THAI/THAI$^+$ include PAR performance behavior as a function of containment thermal-hydraulics, e.g., pressure, temperature, H_2 concentration, steam concentration; PAR performance at O_2-lean atmosphere (initially almost inert conditions); PAR poisoning by fission products (soluble/insoluble aerosol mixture, gaseous iodine); thermal decomposition of CsI to gaseous I_2 (in-containment FP source term); PAR induced-ignition behavior; PAR performance under counter-current flow conditions; and PAR performance under CO and O_2-lean atmosphere.

For experiments, PAR units from AREVA/Framatome (Germany), AECL (Canada), and NIS (Germany) have been used in THAI/THAI$^+$ facility. The variation in test parameters include initial pressure between 0.1 MPa and 0.3 MPa, initial gas temperature between ambient and 117°C; atmosphere steam content of 0–70% (volume fraction); variation in O_2 concentration between 0 and 21% (volume fraction) (air), CO concentration up to 1.5% (volume fraction); and PAR overload by high hydrogen concentration until ignition [28,41].

The performance of the investigated PARs varied regarding PAR start-up behavior. When H_2 was released into an air or steam-air atmosphere, the recombination onset occurred at 0.2%–4.4% H_2 (volume fraction) depending on the initial temperature, pressure, and steam concentration. Experimental data for dry conditions (cases without steam) were within a narrow range but the scattering in PAR start-up was observed for tests with saturated steam. It should be noted that PAR onset occurs for the majority of the tests well within the H_2 concertation value suggested by the PAR vendors except for the cases with PAR exposed to saturated steam. Therefore, despite some spread in minimum H_2 concertation requirement for PAR start-up, PARs indicate quite early onset to control combustible gas related risk far below the lower flammability limit. Furthermore, even if some PAR units are affected by saturated steam (e.g., units located near the leak location), other units distributed in the containment atmosphere shall be able to contribute to the mitigation of combustible gas related risks. The tests conducted with the sequential release of CO and H_2 revealed that under ambient conditions, PAR onset is retarded by CO (in H_2 free atmosphere) and PAR recombination onset does not start until H_2 is injected. However, at elevated temperature (>117°C in THAI tests), PAR onset behavior is not degraded by CO as CO is oxidized by the PAR, even in the absence of H_2.

The test results also showed that the PAR capacity was significantly reduced with the oxygen-to-hydrogen ratio lower than the stoichiometric ratio. The effect of oxygen starvation on hydrogen recombination rate was quantified by using a term "oxygen surplus ratio," defined as $\Phi = 2 \times C_{O_2}/C_{H_2}$. In the used definition of O_2 surplus ratio, C_{O_2} and C_{H_2} are the volumetric oxygen and hydrogen concentrations measured at the PAR inlet. A minimum oxygen surplus ratio (Φ) of 2.2 (AREVA), 2.3 (AECL), and 2.75 (NIS) was required for the PAR to operate at its design capacity. At $\Phi = 1$, the PAR capacity fell below 50% of the design capacity. As shown in Fig. 12, three H_2 recombination regimes are observed during the THAI PAR tests. For an oxygen surplus ratio value $\Phi \leqslant 1$, an O_2-lean and H_2-rich gas mixture exists at the PAR inlet and the rate of oxygen diffusion through the catalyst boundary layer mainly governs the recombination rate. A transition in the hydrogen recombination rate occurs for $1 < \Phi \leqslant 2$, and H_2 recombination is governed by both oxygen and hydrogen diffusion through the catalyst boundary layer. For oxygen surplus ratio value $\Phi > 2$, the H_2-lean and O_2-rich gas mixture prevails at the PAR inlet and the recombination rate is mainly governed by the rate of hydrogen diffusion through the catalyst boundary layer.

The hydrogen depletion efficiency, defined as the ratio

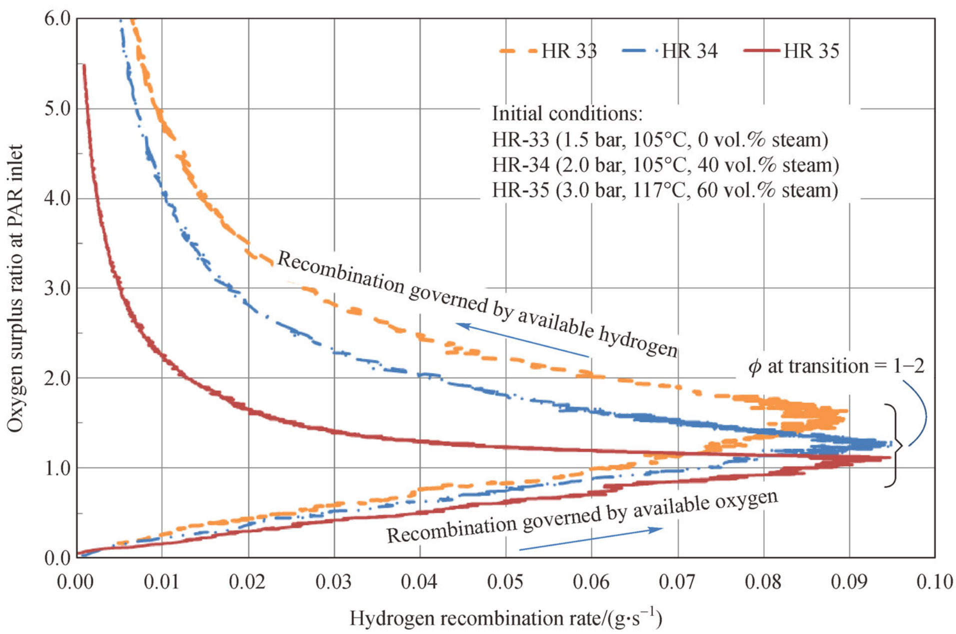

Fig. 12 Hydrogen recombination regimes as observed for AREVA PAR.

of the H_2 concentration difference between the PAR inlet and outlet versus the inlet H_2 concentration, varied between 50–70% in an atmosphere with the oxygen surplus ratio higher than the respective critical value of each PAR. In an oxygen lean atmosphere ($\Phi < 2$), the depletion efficiency was less than 50%, but increased linearly with an increase in the oxygen surplus ratio up to 2 and thereafter remains constant in the aforesaid range of 50%–70%. At higher H_2 concentrations ($V(H_2) > 2\%$, V is volume fraction), the depletion efficiency is independent of the H_2 concentration and decreases with an increase in pressure. It was almost independent of the steam content.

The effect of CO on H_2 depletion efficiency is demonstrated for a test case HR-51 conducted at an initial pressure of 0.15 MPa and a gas temperature of 25°C without steam (Fig. 13). Comparison with another PAR test conducted under the same initial conditions but without CO revealed a slight reduction of the H_2 depletion efficiency under conditions of parallel CO recombination. The efficiency of PAR to oxidize CO is about half of that to oxidize H_2 (Fig. 13). In contrast to H_2, the efficiency of the PAR to recombine CO is not affected by oxygen starvation as long as the O_2 concentration is larger than its stoichiometric demand.

In spite of the benefits associated with the use of PARs as a hydrogen mitigation measure due to its passive nature, there have been some safety concerns owning to PARs tendency to induce ignition. For accident scenarios with excessive hydrogen release rates, some of the PAR units in the containment can reach high operation temperatures, which may cause an ignition of the combustible gas atmosphere. The relevance to reactor safety is the destructive potential of deflagrations with the peak pressures and high temperatures involved. The PAR inlet conditions under which ignition may occur have been determined based on THAI experiments and demonstrate a well-defined range of inlet H_2 concentration, where PARs can ignite (Fig. 14). The ternary diagram depicted in Fig. 14 is based on the air/steam/hydrogen gas mixture system, which needs to be adapted if gas mixture system differs, e.g., for the late phase of MCCI due to reduced O_2 content in air. In the OECD/ NEA THAI-2 project [18], tests were performed with reduced O_2 content in air by establishing gas composition of O_2/N_2/steam at a defined dilution ratio ($\delta = C_{O_2}/(C_{O_2} + C_{N_2})$). The main objective of these tests was to assess the code capabilities to predict PAR ignition potential under transient accident conditions. The data indicate that a change of dilution ratio also modify the steam intertisation limit. In case of a test conducted with a dilution ratio of $\delta = 0.1$ at PAR inlet and a H_2 concentration of 10 vol.%, the inertisation limit of steam concentration was determined to be 30 vol.% instead of 55 vol.% in air/H_2 mixture. It should be noted that the ternary diagram depicted in Fig. 14 is valid for ambient pressure and about 100°C temperature conditions and an increase in gas temperature will further widen the indicated ignition limit on this diagram. The effect of CO addition to H_2-steam-air system on PAR ignition behavior has also been investigated in THAI tests for AREVA-PARs. The test results reveal that PAR induced ignition can be triggered in the presence of CO if the sum of the volumetric concentration of CO and H_2 is larger than the concentration of H_2 which is required to trigger an ignition in absence of CO.

The results are important to assess the possible combustion mode upstream of a PAR by using validated

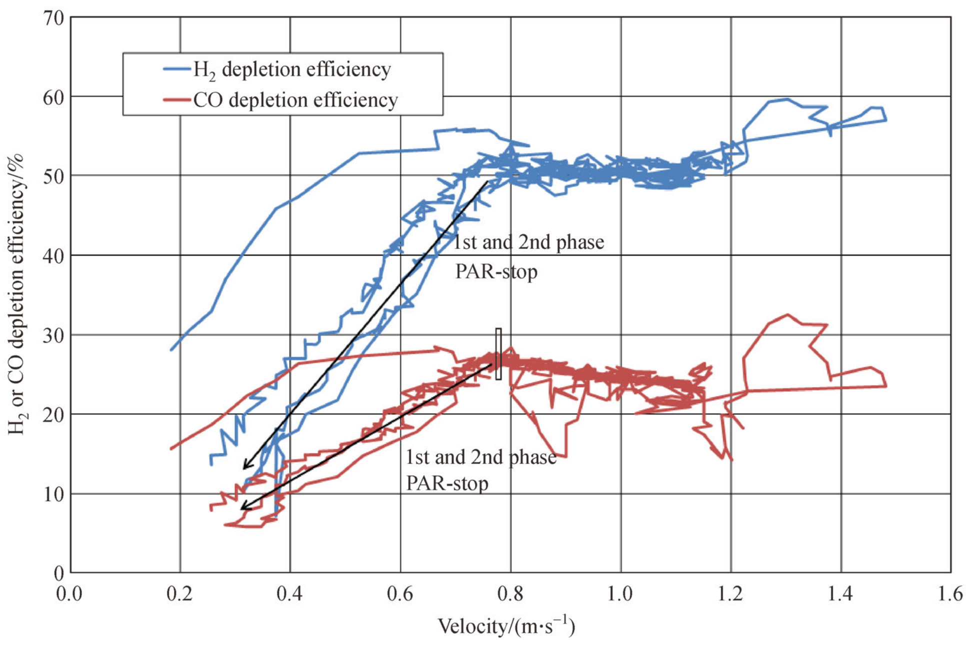

Fig. 13 Test HR-51: H_2 and CO depletion efficiency of a AREVA-PAR.

→ PAR-inlet conditions for the occurrence of an ignition:

✔ Tests in (almost) quiescent atmosphere
✔ O_2 rich atmosphere (surplus > 2.2)
✔ Flammable gas-mixture in the bulk, e.g. steam content < 55 vol.%

Gas atmosphere	Measured catalyst surface temperature (maximum)	Measured H_2 concentration (minimum) at the PAR inlet
Tests without steam	890°C – 920°C	5.5 – 7.5 vol.% H_2 with 0 vol.% steam (depending on the PAR design)
Tests with steam	960°C – 1005°C	8 – 9 vol.% H_2 with 45 vol.% steam

(a)

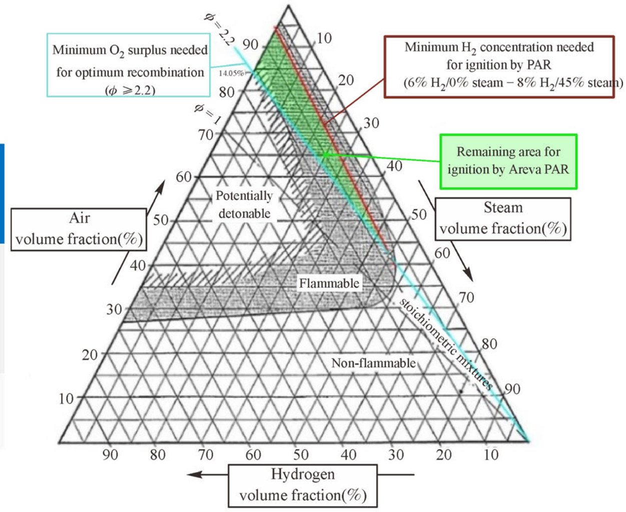

(b)

Fig. 14 PAR induced ignition behavior.
(a) PAR inlet conditions for initiating an ignition in THAI tests; (b) the ternary diagram depicting PAR ignition conditions from THAI tests (adapted with permission from Ref. [17]).

safety analysis tools, or by considering the conditions in probabilistic safety analysis (PSA). The PAR-inducted ignition behavior is also necessary to be considered in full-containment combustion analysis as above PAR location, all the combustion modes are possible for the same accident scenario depending on the available gas composition, geometry, operating safety systems (e.g., spray, cooler, PAR, containment venting), and the prevailing thermal hydraulic conditions (e.g., pressure, temperature, turbulence). Starting as a slow HD near the ignition point, the hydrogen flame can be strongly accelerated if favorable conditions are encountered along its pathway. Therefore, PAR induced ignition and the resulting H_2 deflagration behavior in the surrounding atmosphere provide a basis to assess the severity of a hydrogen explosion which is related to the propagation speed of the deflagration.

Considering long-term operation of PARs, late phase conditions may have an influence on PAR performance and its ignition potential. In oxygen lean mixtures, the concentration of oxygen is the limiting factor for the hydrogen recombination rate and results in lower catalyst temperatures if O_2 starvation conditions are reached. PAR induced ignition potential in O_2 lean mixtures is low, since the catalyst temperatures are directly correlated to PAR self-ignition. Additionally, the presence of CO in the late phase has an influence on PAR recombination capacity as well as its ignition potential as PAR catalyst surfaces may be poisoned by CO under low oxygen conditions, particularly when CO and O_2 concentrations become equal. During THAI tests, it was also observed that the catalyst poisoning is reversible with an increase in H_2 or O_2 concentration.

After ignition, PAR continues to recombine unburned mass of hydrogen available in the gas atmosphere. Tests with continued or restart of hydrogen release shortly after ignition show repetition of PAR induced ignition as soon as favorable conditions for ignition as discussed earlier are met. In one of the THAI "multi-ignition tests," the first two ignitions occurred rather early with an H_2 concentration in the dome area at the lower ignition limit ($V(H_2)$ = 4% for H_2-air mixtures at ambient temperature). Consequently, the deflagration was very smooth and the pressure peak very low. The third ignition occurred at or near the PAR inlet. The flame proceeded first into the vessel bottom zone, and from there upwards into the inner cylinder and annulus zones, and finally into the dome zone. Due to the combustion in the bottom zone with relatively high local H_2 concentration ($V(H_2)$ = 6%) and flame propagation in the entire vessel volume, the pressure increase following the third ignition was higher than that after the previous burns.

One specific feature of the NIS-PAR, which has a different catalyst design as compared to AREVA and AECL PARs, under investigated test conditions with 25% (volume fraction) steam was the expulsion of glowing particles ("glow worms") into the bulk in case of high load ($V(H_2) > 5.2\%$ at the PAR inlet). This visible effect coincided with a marked additional H_2 recombination (in the range of 10% of the total measured recombination) in the bulk without adverse pressure effects. Tests conducted with high steam content (> 40 vol.%) did not show any glow worm. Either "glow worms" did not exist or were not visible due to too low surface temperature. In any case, the higher minimum required ignition energy for the steam-rich mixture could not have been provided.

The performance behavior of an operating PAR when exposed to aerosols and gaseous iodine containing atmosphere under severe accident scenarios is of high significance as it may have an impact on the in-containment FP source term. The details of the two tests on PAR interaction with FP conducted in the OECD/NEA THAI project [17] are shown in Fig. 15. No poisoning was observed if PAR is exposed to FP after the onset of hydrogen recombination and thus rendering catalyst surfaces hot. Combining this finding with the earlier discussed results of O_2 starvation effect, it is possible that during the late phase of the accident involving MCCI, O_2 lean and CO containing atmosphere may lower catalyst surface temperatures but other available heat sources including continuous steam release in containment will keep PAR sufficiently hot to prevent deposition of potential poisons on catalyst surfaces. However, in case of catalyst poisoning and degradation in PAR recombination capacity, PARs may not operate at the design capacity for the purpose of combustible gas risk mitigation. Another investigated issue was related to the possible thermal decomposition of metal iodides passing through an operating PAR. Based on the test results, the decomposition of CsI aerosol to gaseous iodine in the range of 1%–3% was observed. If sufficiently high amount of metal iodides is present in LWR containments, the gaseous iodine produced due to thermal decomposition may increase the FP in-containment source term. Detailed analyses taking into account reactor conditions will be necessary to confirm the impact of measured conversion rate on the potential source term to the environment.

Recently, THAI experimental investigations on PAR performance were extended to accident scenarios in which PAR performance may be adversely affected. One of such scenarios is adverse flow conditions (e.g., counter-current flow) which may have an impact on PAR performance, e.g., delay in start-up or reduction in hydrogen recombination rate and hydrogen depletion efficiency due to possible reduction in PAR induced chimney effect. The effect of counter-current flow was investigated in the THAI$^+$ test facility and the parametric variations included counter-current flow velocity in the vicinity of PAR outlet (0.5 to 1.0 m/s), PAR types (Framatome and NIS), and the PAR chimney height (investigated only for NIS PAR by reducing the height to 50% of the original size). As compared to quiescent atmosphere, no negative impact of the counter-current flow on the start-up as well as the performance of the Framatome PAR was detected under the investigated conditions. The test results of NIS PAR for counter-current flow as compared to quiescent conditions (for the tests with the same chimney height) show a faster start-up but a reduced hydrogen recombination rate and hydrogen depletion efficiency. However, this behavior was observed only for a low hydrogen concentration of about 2.2% (volume fraction). As soon as the H_2 concentration exceeds 2.7% (volume fraction), no adverse influence of counter-current flow on PAR performance could be detected. The NIS PAR with a shorter chimney height showed a reduced performance even at a higher hydrogen concentration. Generally, the results indicate that the top cover plate of the Framatome PAR is an effective design feature to protect the PAR from intrusion of counter-current flow within the range of investigated conditions whereas the open-ended outlet without cover in housing of the investigated NIS PAR is prone to intrusions of counter-current flow. It should be noted that the NIS PARs are commercially available both with and without hood. The NIS PAR unit tested in the THAI test facility under quiescent conditions was without hood and, therefore, to facilitate reference data, counter-current flow tests were also conducted with NIS PAR without hood.

Experimental investigations on PARs are foreseen to be continued in the ongoing OECD/NEA THEMIS project. These PAR tests aim to investigate the influence of H_2-CO-CO_2 containment atmosphere on PAR performance

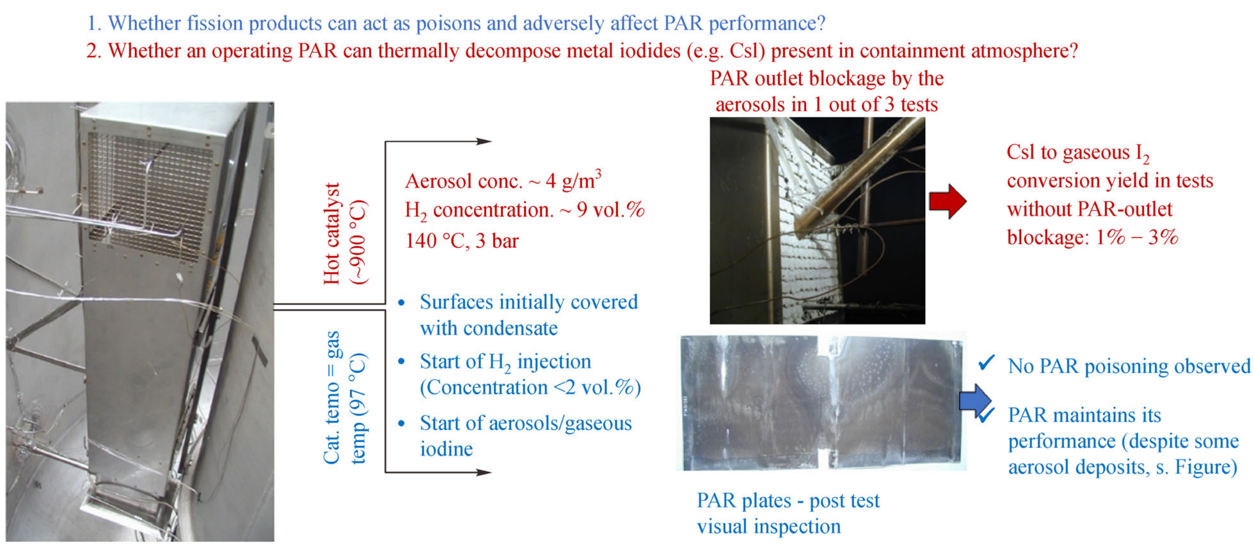

Fig. 15 THAI tests on interaction between an operating PAR and FP.

behavior (e.g., recombination onset, recombination rate, depletion efficiency, PAR poisoning, and PAR induced ignition) under conditions relevant for the late phase of an accident including elevated pressure (up to 0.45 MPa) and the corresponding saturation temperature. In addition, it is envisaged to determine the potential of PAR poisoning by CO in a O_2 lean atmosphere in some tests, and one test is planned with D_2 to investigate PAR performance under conditions typical for a heavy water reactor.

3.3 Water pools

Water pools play an important role in NPPs safety due to the fact that they contribute in pressure suppression by steam condensation as well as by retaining a fraction of FPs from radioactive gas-aerosols mixing passing through it. The retention of FPs in the pool water is of special interest, since it determines the radioactive loading of atmospheric fluid which is passed from the containment gas atmosphere to the environment, either in a controlled manner such as via filtered containment venting system (FCVS) or an uncontrolled release in case of a containment breach or leakage. The state of thermal mixing (homogeneously mixed or thermally stratified pool) may have an influence on FPs release and the retention behavior in water pools. The thermal stratification in the pressure suppression pool of a BWR wetwell has already been subjected to experimental investigations for scenarios involving long lasting accidents (both in-vessel and ex-vessel phase with intact containment) when steam is released through downcomer pipes into the wetwell pool. Other than THAI, other experimental investigations in the PUMA [42] and POOLEX facility [43] also showed that under steam release conditions (post-blowdown), only the pool volume above the downcomer outlet is heated and pronounced thermal stratification can be generated.

A clear understanding of pool hydrodynamics, such as bubble dynamics, pool thermal, and mixing behavior, is essential for the precise calculation of FP retention and release behavior from water pools. THAI experimental research related to water pools cover three main aspects, i.e., pool hydrodynamics, FP release (“re-entrainment”), and FP retention (“pool scrubbing”). A selection of THAI experimental research related to water pools and their main outcomes are described below.

3.3.1 Pool hydrodynamics

A majority of the THAI experimental investigations related to pool hydrodynamics have been oriented toward BWR suppression pool configuration with downscaled 100- or 200-mm diameter downcomer pipe. The tests have been conducted using single-vessel configuration (THAI or PAD). The pool hydrodynamics has been studied in specially devoted test series or as part of FP re-entrainment and pool scrubbing experiments.

For the blowdown phase of an accident, a THAI test series has been oriented toward the water slug phenomena, that is associated with the first few seconds after a large break LOCA in a BWR containment. The fast pressurization of the drywell causes flow through the downcomer pipes into the wetwell pool. The pool dynamics is associated with the formation and acceleration of a water slug, which rises vertically upward from the water surface and may cause mechanical impact forces to the structures in the wetwell air space. If such impact would lead to an opening of pressure relief flaps on the wetwell ceiling, a potential subsequent failure of flap closing would deteriorate the wetwell potential to act as a pressure sink to the steam release from the break. Because of this safety aspect, the determination of potential water slug forces was subject of the THAI blowdown experimental series. The experimental results were aimed to contribute to the validation of related analytical models for safety analyses purpose, e.g., DRASYS, a sub-model of the containment system code COCOSYS. The tests represented the first phase of a blowdown with almost pure air entering the downcomer pipe. All tests were performed at an initial water pool temperature of 14°C and ambient initial pressure. The main parameters to be varied were the downcomer pipe diameter (DN 100 or DN 200) and the blowdown pressure (ranging from 0.3 to 1 MPa).

Figure 16 provides a phenomenology of water slug movement and additionally gives a visual impression of the air bubble dynamics during the blowdown process in the THAI test recoded with a high-speed camera, i.e., Fig. 16(c) downward movement, Fig. 16(d) upward movement after reaching the maximum penetration depth, and Fig. 16(e) pool swelling followed by the outbreak of air bubble above the water surface. After reaching the maximum downward penetration depth, the expanded air bubble displaces the pool free surface upward. The upward water surface motion is driven by the difference between the bubble pressure and the air pressure in the gas space.

The water slug effects investigated in the THAI vessel showed two flow regimes. First, if the initial clearing of the downcomer pipe generates a large flow in the water pool, the gas can spread in the pool without major pressurization. The subsequent rise of the gas bubble generates periodic damped water waves on the pool surface with limited amplitude. Secondly, if there is only small or no water motion generated in the pool during pipe clearing, the gas discharge causes an enhanced pressure in the bubble, which leads to an acceleration and fragmentation of the overlying water layer. Water portions of different sizes are accelerated by the gas to different upward velocities, thus contributing to water slug impact forces with large variability in space and time.

The pool swell velocity is one of the important parameters to evaluate the water slug induced pressure

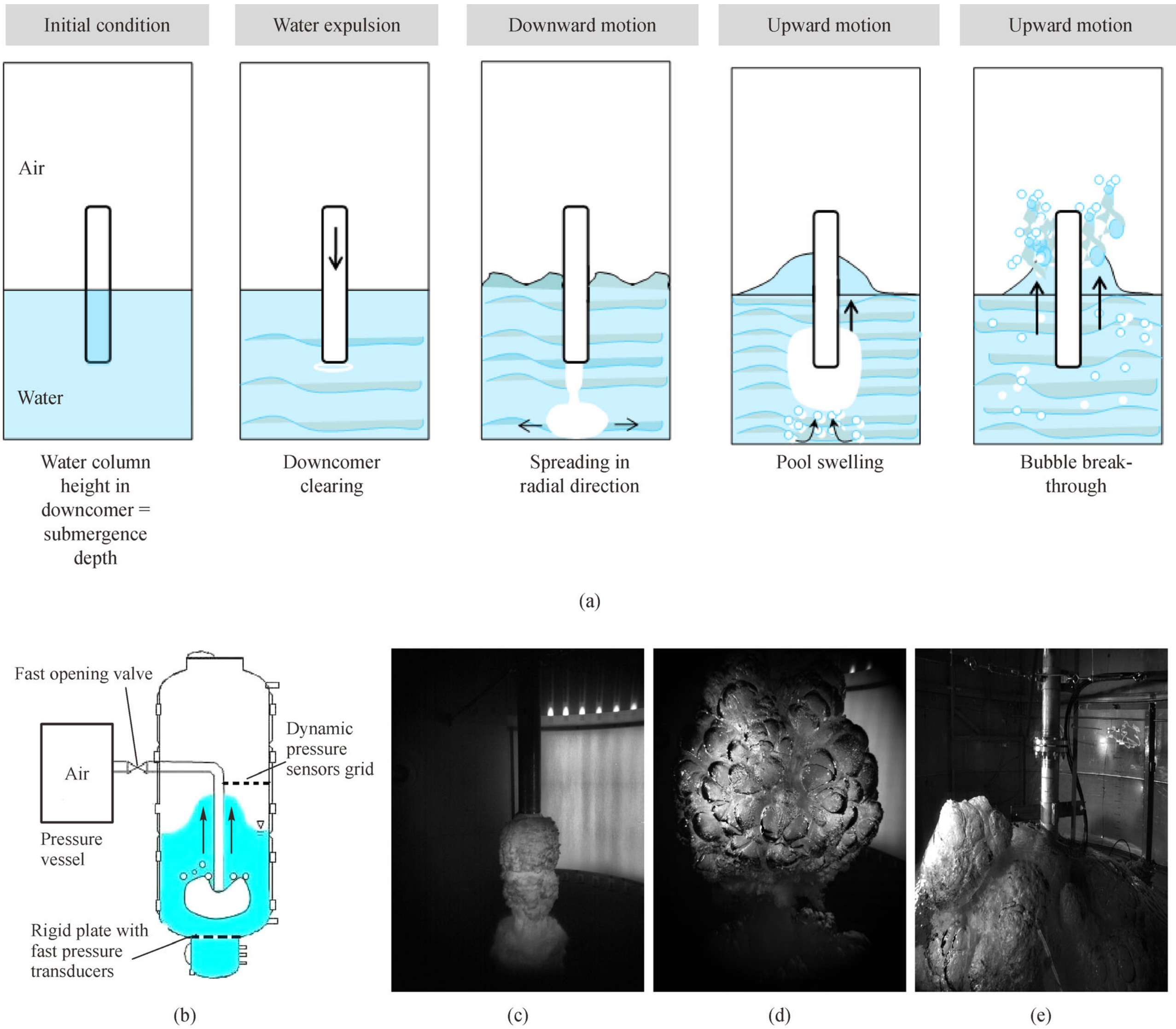

Fig. 16 Air blowdown process in the water pool.
(a) Phenomenology description; (b) test configuration; (c) downward movement; (d) upward movement after reaching the maximum penetration depth; (e) pool swelling followed by the outbreak of air bubble above the water surface.

loadings on the structures and components located within the wetwell. The oscillations of the pressure signals show that the water body is excited to oscillations of a relatively high frequency by the blowdown forces which are transferred to the vessel wall as can be seen from the signals of the strain gauge transducers fixed at the outer surface of the vessel wall. The pressure oscillations and the pool swell velocity as a function of blowdown pressures is shown in Fig. 17 for the test case conducted with a pool height of 5.29 m, a DN 100 downcomer pipe with a submergence depth of 2 m, and a blowdown pressure of 1 MPa. The comparison of tests with different blowdown pressures reveal that the pool swell velocity increase with the increase in the blowdown pressure.

The strongest water slug forces were generated by a slow pipe clearing followed by a large pressure increase in the drywell. Such transient may be associated with a major delay in the leak opening process. In general, the accident transient may involve contributions from both flow regimes, similar to the conditions investigated in the THAI experiments. In summary, it was demonstrated that the acceleration of water in the slug ceases when the air in the pressurized bubble forms channels in the overlying water layer and passes through the layer to the wetwell gas space. The thrust of the water slug is thus governed by the gas discharge from the downcomer, the pool flow pattern associated with the bubble expansion, and the gas release to the gas space.

3.3.2 Bubble dynamics

The bubble dynamics in the water pools has been subject of investigation in several THAI tests. In test series WH 7–15 [44], the test configuration was oriented toward BWR wetwell with a DN 100 downcomer with a submergence depth of 2 m. The tests were performed at atmospheric pressure, and the initial temperature of water in the pool was about 10°C. The air mass flow rate was varied between 10 kg/h and 80 kg/h. A high-speed camera with a frame rate of 1000 fps was used to record the formation and break-up behavior of bubbles at different elevations. The similar experiments conducted at electric power research institute (EPRI) [45] had shown a distinct hydrodynamic behavior of air bubbles in three zones, including rig bubble formation, globules, and near surface bubble dynamics (Fig. 18).

The results of the THAI tests WH 7–15 are widely consistent with the earlier work, e.g., EPRI tests [45] but differ in a specific aspect, the bubble breakup characteristics. In the EPRI tests [45], an extended vertical distance was observed where a continuous transition from large to small bubbles occurred. This distance corresponds to 12 initial globule diameters. In contrast to this, the present data show a rapid transition from large to small bubbles above the downcomer pipe exit. This difference may be caused by the relatively larger initial globules generated in the WH 7–15 tests [44] which implies relatively larger buoyancy forces driving the globule decay processes.

The process of ring bubble formation at the downcomer outlet repeats itself at a characteristic frequency. In the THAI experiments conducted under ambient pressure conditions, combining all results, a mean formation frequency of 4.2 Hz was found. This can be compared with the results in Ref. [45] where two mean formation frequencies of 2.8 Hz and 1.4 Hz for downcomer pipe diameters of 0.15 m and 0.6 m are found. Including the present result of f = 4.2 Hz with a downcomer pipe diameter of D = 0.1 m, the variation of the ring bubble formation frequency f with the downcomer diameter can approximately be correlated as expressed in Eq. (3).

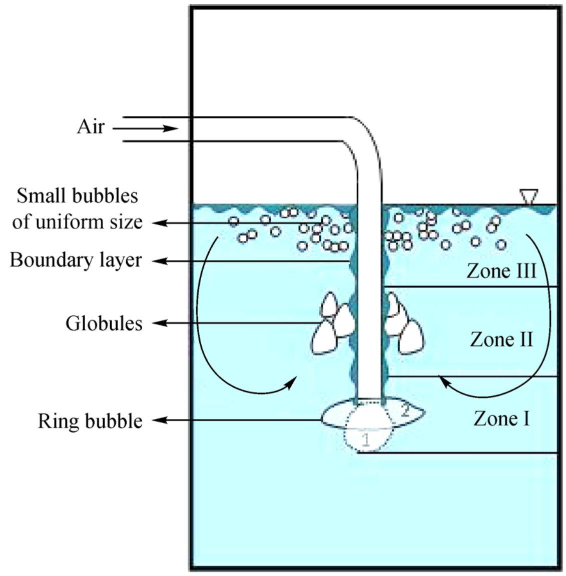

Fig. 18 Schematic of bubble column dynamics in the water pool.

$$f = 0.1 \times \sqrt[3]{\frac{\sigma g}{\eta D^2}}, \tag{3}$$

where g is the gravitational acceleration, σ the surface tension, and η the dynamics viscosity of the water; f is calculated in units of Hz. This correlation and the frequencies for THAI tests ("present study") and Paul et al. [45] are plotted together in Fig. 19.

The correlation represents the experimental data well and shows the consistency of the present results with the earlier data in Ref. [45]. Both test series show that the formation frequency is practically independent of the air

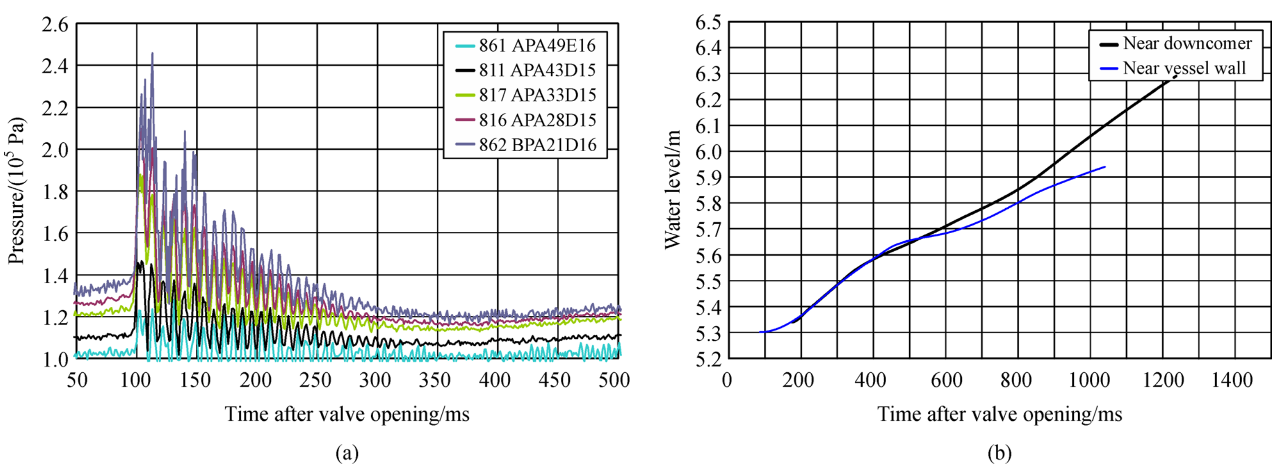

Fig. 17 Test case with blowdown pressure of 1 MPa.
(a) Pressure oscillations in water pool; (b) pool swelling velocity.

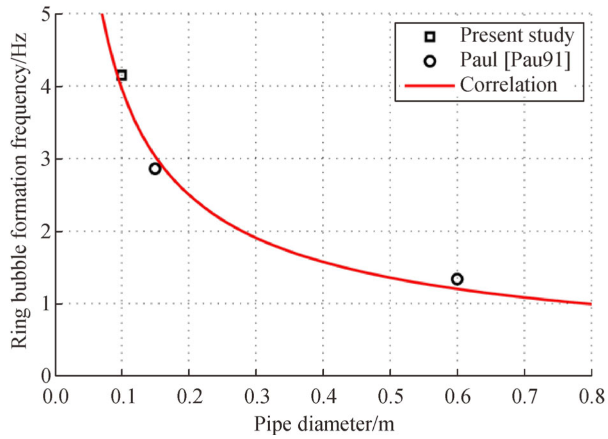

Fig. 19 Ring bubble formation frequencies for different downcomer pipe diameters.

flow rate. Furthermore, the correlation indicates a plausible dependency upon the material properties σ and η and the gravitational acceleration g, and it allows upscaling to a larger downcomer diameter.

The recently conducted tests in the framework of OECD/NEA THAI-3 [19], further extend the parameter range as well as boundary conditions aiming to cover representative severe accident conditions by conducting the tests at an elevated pressure/temperature, including steam. The effect of elevated pressure/temperature conditions on bubble dynamics is demonstrated in Fig. 20. With respect to bubble dynamics, some differences, such as primary bubble formation frequency and its maximum ascending height before break-up into globules, and bubble size at water surface are observed between the present results and the literature (e.g., EPRI tests [45]). In the near-surface zone, which exists far away from the pipe outlet in the vicinity of the water surface, the liquid turbulence further breaks-up the large globules into small bubbles of approximately uniform diameters in the range of 4–6 mm and independent of the injected gas flow rate are measured under ambient conditions, e.g., Refs. [44,45]. The tests at a higher initial pressure (0.25 MPa) revealed a reduction in the bubble size near the surface. Similar to the WH 7 – 15 tests, THAI tests conducted at elevated pressure also did not show a cascaded reduction of bubble sizes from initially large structures into smaller and smaller as observed in EPRI experiments [45], instead a complete break-up of primary bubble occurs within shorter distance from the downcomer outlet. The most significant difference between the OECD/NEA THAI-3 tests and the EPRI test [45] are the temperature of the water pool and the pressure above the water surface-EPRI tests being performed at ambient pressure using cold water (20°C). The results indicate that model assumptions derived from air bubble measurements at ambient pressure and temperature conditions need adoptions for representative boundary conditions as expected in the course of a postulated severe accident.

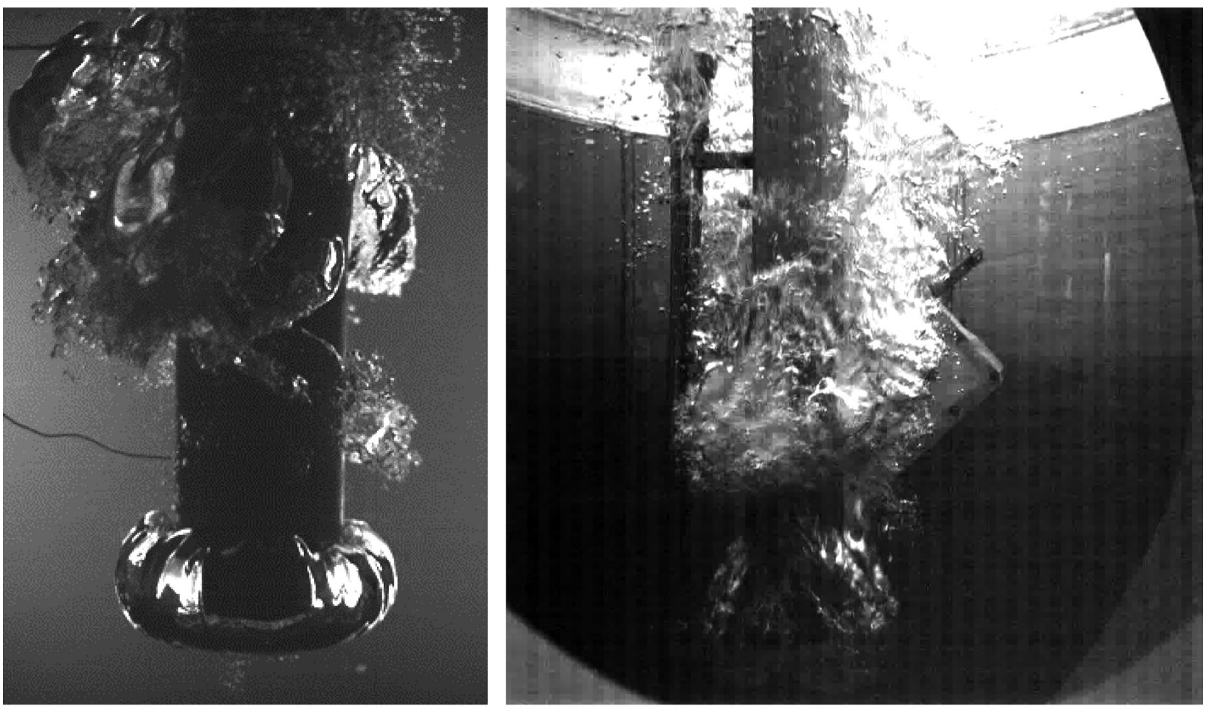

(a) (b)

Fig. 20 Bubble dynamics in water pools.
(a) Ambient pressure/temperature, without steam; (b) elevated pressure/temperature condition, with steam.

3.3.3 FPs release from water pools ("Re-entrainment")

The re-entrainment of droplets from water pools containing suspended or dissolved FPs can have a significant contribution to the source term [46]. Such re-entrainment processes from water pools are expected, e.g., if the containment sump or another water pool in the containment starts boiling by continuous heat input (decay heat) and/or pressure reduction (e.g., during containment venting), by gas flow though water pools (e.g., pool scrubbing), or in a flooded pool of molten core material. As re-entrainment can contribute to the source term by providing long-term release sources of FPs, the re-entrained fraction of FPs may play a vital role in SAM measures (e.g., timing of FCVS operation) and in determining the source term to the environment.

In the THAI experiments, the re-entrainment of aerosols from water pools have been investigated in tests by using aerosol materials of different chemical natures: CsI, CsCl, KI, Cs_2SO_4, and Li_2SO_4 salts as soluble aerosols, and non-soluble aerosol suspension of calcium carbonate ($CaCO_3$) with two different primary mass-median diameters of 0.065 μm and 0.9 μm. The tests have been performed either using a test configuration allowing release of uniform bubbles from perforated tubes in the pool [47], or by employing a BWR wetwell typical configuration with a downcomer [19]. The re-entrainment was affected either by injecting steam or steam/air mixtures at the bottom of the water pool or by depressurization induced boiling. The investigated superficial velocities (defined as the volume flow of the released gas and steam bubbles per unit area of the pool) ranged from 0.024 m/s to 0.13 m/s with higher values representing the churn turbulent flow regime. The re-entrainment rates were measured based on different measurement techniques [19,47]. The results from selected THAI tests conducted with soluble aerosols are shown in Fig. 21 [47]. The entrainment factor E (dimensionless) is the ratio of the mass flow of released droplets above the pool to the gas- and steam mass flow released into the water pool, respectively. For soluble aerosols, the re-entrainment rates were determined to be varying between 5×10^{-6} and 1×10^{-4}. To mimic the reactor typical water boundary conditions during an accident, a test was conducted with surfactants reducing the surface tension of the water. The soluble aerosol re-entrainment in the test with surfactant was one order of magnitude higher compared to the test without surfactant. The results from different particle measurement techniques which have been used to evaluate the entrainment in THAI tests, indicate that the absolute entrainment are subject to an uncertainty by a factor of 2–5.

Regarding the differences in the release behavior between soluble and insoluble aerosols, it is typically assumed that the concentration of soluble matter is the same in the released droplet as in the pool. For insoluble matters, higher concentrations in the droplets than in the pool have been reported, meaning an enrichment of insoluble matter in the droplets [48,49]. Although this enrichment leads to a larger resuspension in terms of absolute mass, it might in contrary lead to a faster settling of the larger particles. Similar trend was observed in the THAI tests conducted with insoluble aerosol $CaCO_3$, and

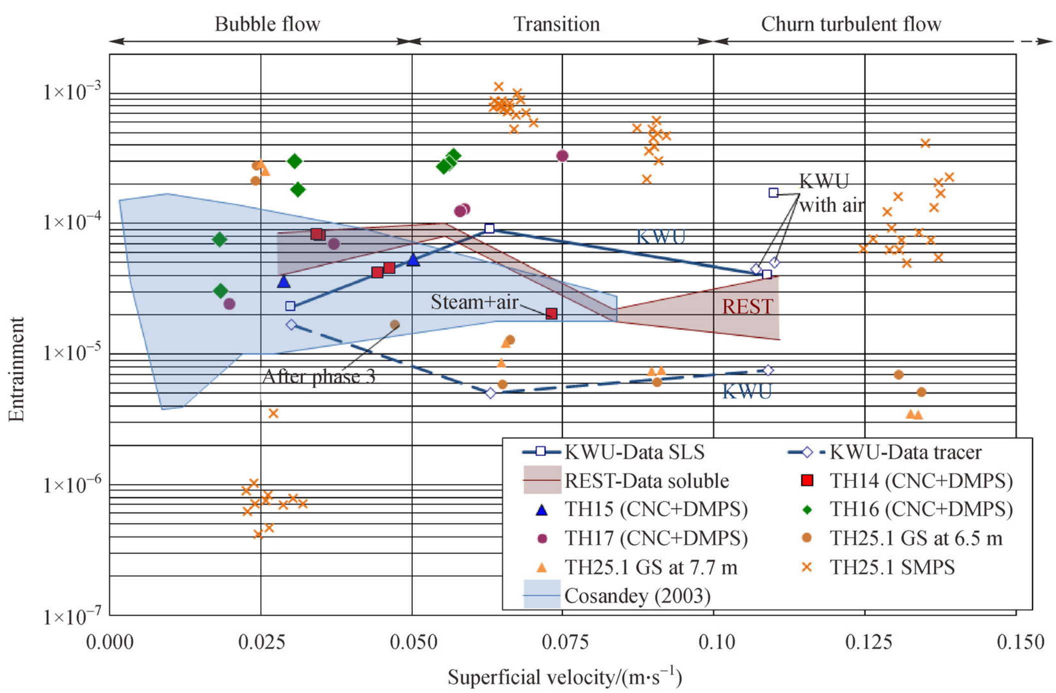

Fig. 21 Measured entrainment in THAI tests and comparison with literature for soluble aerosols (reproduced with permission from Refs. [13,47]).

the measured aerosol enrichment was between 1.6 and 7 of non-soluble aerosol concentration inside the droplet being released from the sump [47]. Former findings of the REST experiments [48] reported an enrichment coefficient of 20 for insoluble aerosols, for a similar range of superficial velocities but different chemical compositions of aerosols in the sump water.

Another safety relevant insight from experiments was regarding the characteristics of the aerosols released from water pools. The test results indicate that mainly very small aerosols (sub-micron range) are released from a boiling pool, which in turn might remain airborne for a long time. Such a small particle size represents an unfavorable value for the design of the accident management measure filtered containment venting because filters normally show a minimum efficiency in this particle size range (“filter gap”).

3.3.4 FPs retention in water pools (“pool scrubbing”)

The topic of pool scrubbing plays a vital role in mitigating the source term to the environment by retention of FPs passing through water pools. The retention behavior of volatile iodine species (e.g., molecular iodine, organic iodide) and aerosols of different chemical nature (soluble or insoluble) in water pools is governed by complex processes as well as mass-transfer characteristics in gas-liquid two-phase conditions. The retention efficiency of aerosol particles in water pools is calculated in terms of “decontamination factor (DF)” defined as the ratio of particle mass entering into the pool to the particle mass escaping in the gas space above the water pool. The majority of the experimental studies related to pool scrubbing were conducted in 1980s/1990s in order to establish suitable models for predicting the pool decontamination efficiencies under reactor-typical conditions. The results from past research on pool scrubbing showed that both experimental data on aerosol retention in water pools as well as related model predictions were affected by large uncertainty bands which make application to reactor cases questionable. Among others, the hydrodynamic behavior in the water pool and the effect of aerosol material chemical nature, chemical conditions (e.g., pH, impurities), saturated water pool, and submerged structures, on pool scrubbing processes was not very well understood. In this context, an international collaboration project integration of pool scrubbing research to enhance source-term calculations (IPRESCA) [5] is currently underway with an aim to promote a better integration of international research activities related to pool scrubbing by providing support in experimental research to broaden the current knowledge and database, and by supporting analytical research to facilitate systematic validation and model enhancement of the existing pool scrubbing codes. The THAI experiments on pool scrubbing also contribute to the analytical activities being performed in the IPRESCA [5] framework.

The THAI experiments investigating aerosols pool scrubbing (test series WH 25 – 27, Table 3) have been conducted using a test configuration representative of BWR wetwell and using insoluble SnO_2 as test aerosols. The test matrix included 13 different conditions including, pool scrubbing from a pre-heated pool by injection of air and steam/air mixtures, pool scrubbing from a strongly heated pool by injection of air and steam/air mixtures, and pool scrubbing from a quasi-boiling pool by injection of air and steam/air mixtures [50]. The main test parameter variations included initial vessel pressure (0.2 – 0.35 MPa),

Table 3 Average test conditions as measured during the phases of test series WH-25 to WH-27 (The bracketed values refer to the condition at the beginning of the corresponding phase—Part 1)

Test	Phase	Vessel pressure /(10^{-1} MPa)	Air injection /($g \cdot s^{-1}$)	Steam injection /($g \cdot s^{-1}$)	Steam mass fraction /%	Water temperature /°C	Purge air /($kg \cdot h^{-1}$)
WH-25	0.1	2	4	0	0	60	10
WH-25	0.2	2	2	2	50	60	10
WH-25	0.3	3.5	4	0	0	60	20
WH-25	0.4	3.5	2	2	50	60	20
WH-26	0.1	2	2	2	50	105	10
WH-26	0.2	2	4	4	50	105	10
WH-26	0.3	2	6	6	50	105	10
WH-26	0.4	2	8	8	50	105	10
WH-27	0.1	3.5	2	2	50	105	20
WH-27	0.2	3.5	2	6	75	105	20
WH-27	0.3	2	2	6	75	105	10
WH-27	0.4	2	2	6	75	Boiling	10
WH-27	0.5	3	2	6	75	Boiling	20

Table 4 Average test conditions as measured during the phases of test series WH-25 to WH-27 (The bracketed values refer to the condition at the beginning of the corresponding phase—Part 2)

Test	Phase	Gas mass flux/($g\cdot s^{-1}m^{-2}$)	Injection weber number	Injection weber number, air only
WH-25	0.1	127	8.3	8.3
WH-25	0.2	127	14.9	2.1
WH-25	0.3	127	2.9	2.9
WH-25	0.4	127	5.2	0.7
WH-26	0.1	127	19.5	3.0
WH-26	0.2	255	78.0	11.8
WH-26	0.3	382	175.5	26.6
WH-26	0.4	509	311.9	47.3
WH-27	0.1	127	6.9	1.0
WH-27	0.2	255	37.3	1.0
WH-27	0.3	255	106.0	3.0
WH-27	0.4	255	113.7	3.3
WH-27	0.5	255	43.7	1.4

water pool temperature (60°C – 130°C), and injection weber number for air or air/steam mixtures (3 – 240). One additional test was performed without water body to characterize the particle segregation by particle sedimentation and diffusive separation without pool scrubbing.

The injection weber number at the exit of the downcomer, according to Paul et al. [45] is defined by

$$We = u_0^2 \times \left(\frac{\rho_w D_0}{\sigma}\right), \tag{4}$$

where ρ_w is the water density, u_0 is the gas injection velocity, D_0 is the downcomer diameter, and σ is the surface tension of the pool water.

As shown in Fig. 22(a), the range of measured DFs was between 10 and 170, the test without water with a DF of 8. The measurement uncertainty of the DF showed an exponential increase with an increase in DF, indicating larger DF values are subject to larger measurement uncertainties (Fig. 22(b)). The well-profound correlation coefficients were determined for the injection particle diameter, the air flow rate, and the amount of condensing steam. Thereby, the large particle diameter and high steam condensation enhance the particle segregation whereas high air flow rates reduce the corresponding DF.

In these tests, the superficial gas velocity was between 0.5 – 0.08 m/s, corresponding to the bubble flow regime. In addition to DF measurements, the gas release from the downcomer and the bubble column were measured by high-speed digital imaging to provide needed database on pool hydrodynamics for validation and further improvement of pool scrubbing modeling.

The pool scrubbing investigations continue to be part of the THAI experimental research. In the ongoing OECD/NEA THEMIS project, pool scrubbing experiments using insoluble aerosols are planned under the jet-regime condition. Limited data are available for the jet injection regime which is characterized by high weber numbers ($>10^5$) of the injected gas. In contrast to the low weber number regime of pool scrubbing where the deposition mostly happens at the bubble surface, the main deposition is expected to be attributed to capture at liquid droplets entrained into the gas jet. The planned tests in the THAI vessel will allow jet injection with a large distance from the injection nozzle to the opposite vessel wall for minimizing wall effects on the gas jet.

4 Conclusions and perspectives

An overview of the THAI experiment research related to containment safety system performance behavior as well as effects of their operation on H_2 risk and in-containment FPs behavior has been provided. The main insights obtained from the experiments conducted in the THAI/THAI$^+$ test facility related to containment spray, PARs, and water pools are summarized.

The outcomes of spray tests have shown an overall beneficial effects of spray operation on controlling containment pressure-temperature, and in mitigation of potential in-containment source term by reducing the gas borne FPs concentration. The observed effects of efficiency degradation in depletion of sub-micron aerosol particles as well as the effect of spray induced turbulence on combustion behavior should be taken into consideration for containment safety analyses and source term related investigations.

The THAI PAR test results enlarged the knowledge on the start-up behavior, performance, and ignition potential

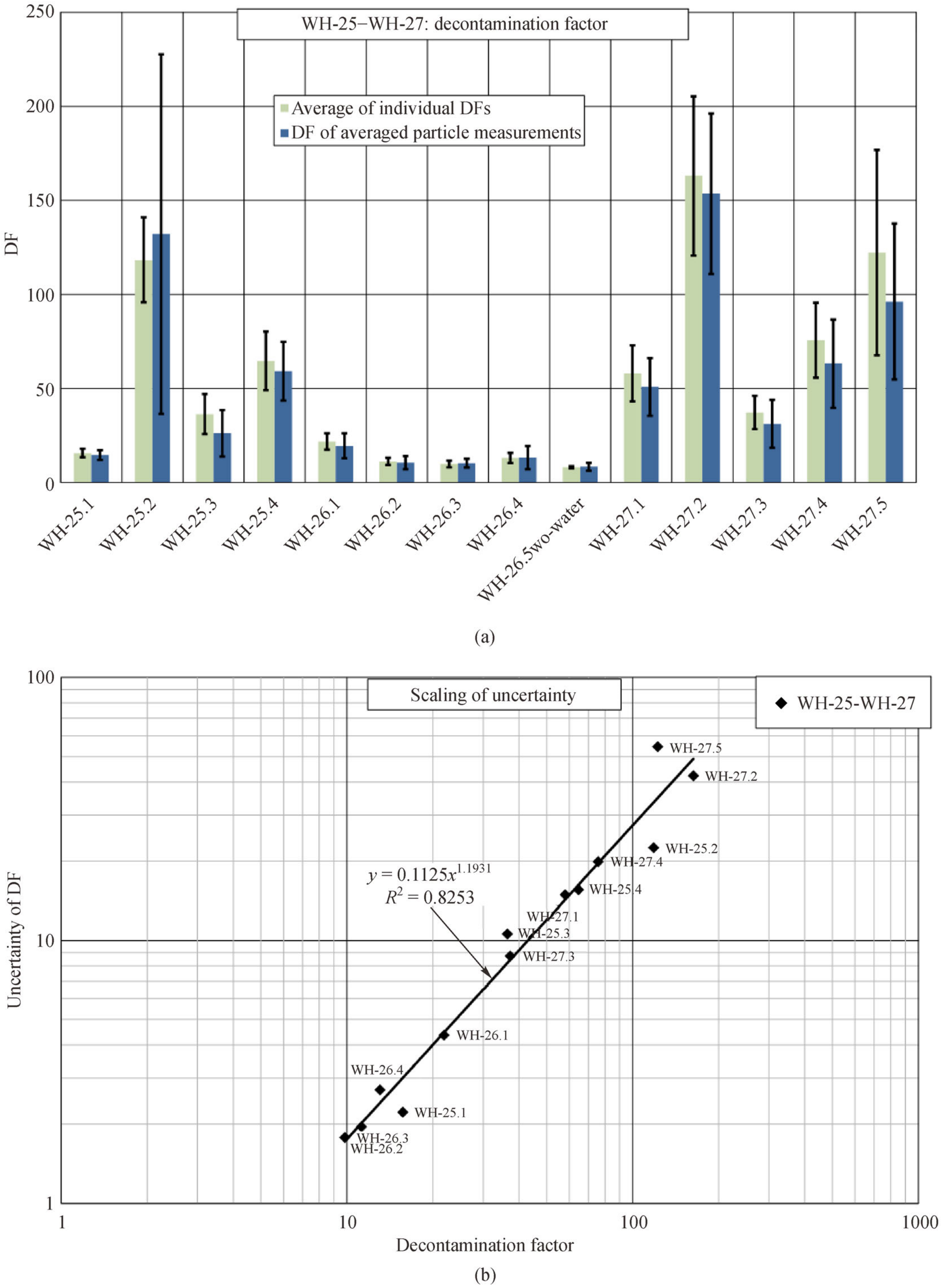

Fig. 22 Decontamination factors and uncertainties of the individual test phases.
(a) Distribution of decontamination factors; (b) corresponding uncertainties of the individual test phases.

under severe accident conditions and provided useful information for PAR model validation for CFD, LP, and mechanistic codes in addition to the data gained from earlier experiments. The experimental database includes PAR performance under “oxygen starvation” conditions as well as at a CO containing atmosphere as expected during the late phase of an accident. The safety relevant aspects related to PAR operation are PAR self-ignition and the effect of an operating PAR (elevated catalyst surface temperature) on the source term, e.g., due to the thermal decomposition of metal iodide aerosols. These aspects require to be taken into consideration in containment safety analyses. On the other hand, some phenomena like, PAR catalyst poisoning under O_2 lean and CO containing atmosphere, are still not well understood and future work is necessary with an emphasis on late phase conditions, which might have an impact on the PAR system installation methodology (e.g., number of PARs).

The experimental research on water pools in the THAI projects is oriented toward water pool hydrodynamics, fissions products release (re-entrainment), and FP retention ("pool scrubbing"). WH related investigations carried out under severe accident typical conditions (e.g., elevated pressure, steam, impurities) have significantly enhanced both phenomenological understanding as well as database for the code validation purpose particularly related to the bubble dynamics behavior. The physical and chemical characteristics of released aerosols (e.g., very fine particles) need to be considered in SAM analyses, e.g., due to the degraded retention efficiency of the FCVS system for very fine particles ("filter-gap"). Even though important insights have been gained from THAI project data, the experiments conducted have only partly covered relevant boundary conditions and the database needs to be extended to the wider range conditions anticipated during a postulated severe accident, including the effect of flow regimes (bubble to churn turbulent), representative chemical boundary conditions (e.g. impurities), representative gas composition, elevated pressure/temperature, high velocity flows, etc.

In summary, the THAI experimental results provide suitable database for validation of severe accident analyses tools and input to validate SAM measures, e.g., by providing a spectrum of accident scenarios for consideration in PSA studies to get a global view of potential risks and possibilities for safety improvements by means of improvements in SAM procedures. Some of the remaining open issues related to FP and combustible gas behavior are being considered in the ongoing international projects, e.g., SNETP-NUGENIA in-kind projects IPRESCA and SAMHYCO-NET, EC funded project AMHYCO. Regarding THAI projects, the recently launched OECD/NEA THEMIS project (2020–2024) focuses on the "late phase" conditions of severe accidents, e.g., reduced O_2 concentrations, presence of CO, and representative FPs. Topics related to combustible gas include hydrogen/carbon monoxide combustion and PAR performance behavior. Other topics planned to be investigated include pool scrubbing under jet-regime, iodine oxide behavior under high temperature conditions and its interaction with other nuclear aerosols. The project aims shall contribute to better understanding of the severe accident-related phenomenology, produce new database for code validation and development purpose, and provide contribution to optimisation of SAM measures. The current phase of the THAI national project (Phase-VII) focuses on thermal-hydraulics, combustible gases, and FPs related research for existing NPP designs. The national THAI VII project also aims to cover thermal-hydraulic issues oriented toward water-cooled small modular reactors.

Acknowledgements THAI experimental research program is funded by the German Federal Ministry for Economic Affairs and Energy, on the basis of a decision of the German Bundestag. The sponsorship by the countries of the OECD/NEA THAI, THAI-2, THAI-3 and the ongoing THEMIS projects is gratefully acknowledged.

Notations

AICC	Adiabatic Isochoric Complete Combustion
AIM	Advanced Iodine Model
APR	Advanced Power Reactor
AW	Aerosol Washdown
BMC	Battelle Model Containment
BMWi	Bundesministerium für Wirtschaft und Energie (German Federal Ministry for Economic Affairs and Energy)
BWR	Boiling Water Reactor
CFD	Computational Fluid Dynamic
COCOSYS	Containment Code System
CSNI	Committee on the Safety of Nuclear Installations
DBA	Design Basis Accident
FCVS	Filtered Containment Venting System
FP	Fission Product
GRS	Gesellschaft für Anlagen- und Reaktorsicherheit
HD	Hydrogen Deflagration
HR	Hydrogen Recombiner
Iod	Iodine
IPRESCA	Integration of Pool Scrubbing Research to Enhance Source-term Calculations
LDA	Laser Doppler Anemometer
LOCA	Loss of Coolant Accident
LP	Lumped Parameter
LWR	Light Water Reactor
MCCI	Molten Corium Concrete Interaction
METUSA	Minimal Encroaching Turnable Streamwise Anemometers
MMD	Mass Median Diameter
NEA	Nuclear Energy Agency
NPP	Nuclear Power Plant
OECD	Organisation for Economic Co-operation and Development
PAD	Parallel Attachable Drum
PAR	Passive Autocatalytic Recombiner
PIV	Particle Image Velocimetry
PWR	Pressurized Water Reactor
RCS	Reactor Coolant System

SAM	Severe Accident Management
SMD	Sauter Mean Diameter
TH	Thermal- Hydraulic
THAI	Thermal-hydraulics, Hydrogen, Aerosols, and Iodine
THEMIS	THAI Experiments on mitigation measures, and source term issues to support analysis and further improvement of severe accident management measures
TMI	Three Mile Island
TTV	THAI Test Vessel
VVER	Voda Voda Energo Reactor (Water-Water Energetic Reactor)
WGAMA	Working Group on Analysis and Management of Accidents
WH	Water Hydrodynamic

References

1. International Atomic Energy Agency. Developments in the analysis and management of combustible gases in severe accidents in water cooled reactors following the Fukushima Daiichi accident. Report: IAEA-TECDOC-1939, 2020
2. NEA. CSNI/WGAMA source term workshop 2019. Report: NEA/CSNI/R (2020)4, 2020
3. Cheng X, Wielenberg A, Hampel U, et al. Summary of 3rd Sino-German symposium on fundamentals of advanced nuclear safety technology. Kerntechnik, 2020, 85(2): 131–135
4. Bentaib A. SAMHYCO-NET overview. In: Proceedings of the International Workshop on Hydrogen Safety for Nuclear Power Plants 2019, Fontenay-aux-Roses, 2019
5. Gupta S, Herranz L E, Van Dorsselaere J. Integration of pool scrubbing research to enhance Source Term calculations. In: Proceedings of 8th European Review Meeting of Severe Accident Research (ERMSAR) 2017, Warsaw, Poland, 2017
6. Herranz L E, Bentaib A, Gabrielli F, et al. NUGENIA/TA2 achievements in severe accidents research (2015–2020). Journal of Nuclear España, 2020, 2020: 1–6
7. Gupta S, Schmidt E, von Laufenberg B, et al. THAI test facility for experimental research on hydrogen and fission product behaviour in light water reactor containments. Nuclear Engineering and Design, 2015, 294: 183–201
8. Kanzleiter T, Ahrens G, Fischer K, et al. Experimental facility and program for the investigation of open questions on fission product behaviour in the containment, Part 1: test facility and thermal-hydraulic experiments. Report: 150 1218–S1, 2003
9. Funke F, Greger G U, Langrock G, et al. Experimental facility and program for the investigation of open questions on fission product behaviour in the containment, Part 2: iodine experiments. Report: 150 1218–S2, 2004
10. Kanzleiter T F, Ahrens G, Fischer K, et al. Experimental facility and program for the investigation of open questions on fission product behaviour in the containment, ThAI Phase II, Part 1: test facility, thermal-hydraulic and aerosol experiments. Report: 150 1272–S1, 2007
11. Funke F, Langrock G, Kanzleiter T, et al. Experimental facility and program for the investigation of open questions on fission product behaviour in the containment, ThAI Phase II, Part 2: iodine experiments. Report: NTR-G/2007/de/0233A, 2006
12. Kanzleiter T, Fischer K, Langer G, et al. Test program on fission product and hydrogen behaviour in containment, THAI-III-National-1. Report: 1501325-III-N1, 2009
13. Gupta S, Balewski B, Freitag M, et al. Experimental program on source-term relevant phenomena in the containment and for further development and validation of models-THAI IV. Report: 1501361-FR, 2013
14. Gupta S, Freitag M, Schmidt E, et al. Single- and multi-compartment tests on fission- product and hydrogen behaviour in the containment-THAI-V. Report: 1501455-FR, 2017
15. Gupta S, Poss G, Freitag M, et al. Experimental investigations on fission-product retention and hydrogen mitigation for design-basis and severe accidents in the containment-THAI VI. Report: 1501547-FR, 2019
16. Gupta S, Poss G, Freitag M, et al. Experimental investigations on fission-product retention and hydrogen mitigation for design-basis and severe accidents in the containment-THAI VI-b. Report: 1501594-FR, 2021
17. OECD/NEA THAI Project. Hydrogen and fission product issues relevant for containment safety assessment under severe accident conditions. OECD/NEA THAI Project Final Report: NEA/CSNI/R (2010)3, 2010
18. OECD/NEA THAI-2 Project. Aerosol and iodine issues, and hydrogen mitigation under accidental conditions in water cooled reactors. Thermal-hydraulics, Hydrogen, Aerosols and Iodine (THAI-2) Project Final Report: NEA/CSNI/R(2016)8, 2016
19. Gupta S, Poss G, Freitag M, et al. Fission product behaviour, hydrogen mitigation, and hydrogen combustion in water cooled reactors under severe accident conditions. OECD/NEA THAI-3 Project Final Report: 1501516-FR-1, 2020
20. Nuclear Energy Agency. THAI experiments on mitigation measures, and source term issues to support analysis and further improvement of severe accident management measures (THEMIS) project. 2021–6-4, available at website of NEA
21. Gupta S, von Laufenberg B, Freitag M, et al. Instrumentation for LWR containment experiments under accident conditions. In: Proceedings of Specialist Workshop on Advanced Instrumentation and Measurement Techniques for Nuclear Reactor Thermal Hydraulics (SWINTH-2016), Livorno, Italy, 2016
22. Freitag M, von Laufenberg B, Colombet M, et al. Challenges and uncertainties in providing validation data for fission product transport modelling. In: Proceedings of ANS Best Estimate Plus Uncertainty International Conference (BEPU 2018), Lucca, Italy, 2018
23. Freitag M, von Laufenberg B, Poss G. Development and application of an online spectroscopy based gas concentration measurement system applicable for gaseous iodine and steam concentration. In: Proceedings of OECD/NEA Specialist Workshop on Advanced Measurement Method and Instrumentation for Enhancing Severe Accident Management in an NPP addressing Emergency, Stabilization and Long-term Recovery Phase (SAMMI), 2020
24. Schwarz S, Fischer K, Bentaib A, et al. Benchmark on hydrogen distribution in a containment based on the OECD-NEA THAI HM-2

experiment. Nuclear Technology, 2011, 175(3): 594–603
25. Allelein H J, Fischer K, Vendel J, et al. International standard problem ISP-47 on containment thermal hydraulic. Report: NEA/CSNI/R(2007)10, 2007
26. Freitag M, Schmidt E, Gupta S, et al. Simulation benchmark based on THAI-experiment on dissolution of a steam stratification by natural convection. Nuclear Engineering and Design, 2016, 299: 37–45
27. Freitag M, Kljenak I, Jankowski T, et al. Benchmark exercise TH-27 on natural convection with steam injection and condensation inside the extended THAI facility. Annals of Nuclear Energy, 2018, 116: 90–104
28. Gupta S, Freitag M, Liang Z, et al. Main outcomes and lessons learned from THAI passive autocatalytic recombiner experimental research and related model development work. In: Proceedings of 17th International Topical Meeting on Nuclear Reactor Thermal Hydraulics (NURETH-17), Xi'an, China, 2017
29. NEA. ISP-49 on hydrogen combustion 2012. Report: Nuclear Safety NEA/CSNI/R(2011)9, 2011
30. Weber G, Bosland L, Funke F, et al. ASTEC, COCOSYS, and LIRIC interpretation of the iodine behaviour in the large-scale THAI test Iod-9. In: Proceedings of 17th International Conference on Nuclear Engineering, Brussels, Belgium, 2010: 519–531
31. Funke F, Langrock G, Kanzleiter T, et al. Iodine oxides in large-scale THAI tests. Nuclear Engineering and Design, 2012, 245: 206–222
32. Weber G, Herranz L E, Bendiab M, et al. Thermal-hydraulic-iodine chemistry coupling: insights gained from the SARNET benchmark on the THAI experiments Iod-11 and Iod-12. Nuclear Engineering and Design, 2013, 265: 95–107
33. Gupta S, Funke F, Langrock G, et al. THAI experiments on volatility, distribution and transport behaviour of iodine and fission products in the containment. International Iodine Workshop Summary Report Nuclear Safety: NEA/CSNI/R(2016)5, 2016
34. Funke F, Gupta S, Weber G, et al. Interaction of gaseous I_2 with painted surfaces and aerosols in large-scale THAI tests. International Iodine Workshop Summary Report: Nuclear Safety NEA/CSNI/R(2016)5, 2016
35. Weber G, Funke F, Klein-Hessling W, et al. Iodine and silver wash-down modelling in COCOSYS-AIM by use of THAI results. International Iodine Workshop Summary Report: Nuclear Safety NEA/CSNI/R(2016)5, 2016
36. Wang F, Cheng X, Gupta S. COCOSYS analysis on aerosol wash-down of THAI-AW3 experiment and generic containment. Annals of Nuclear Energy, 2021, 153: 108076
37. Gupta S, Schmidt E, Freitag M, et al. Experimental investigations on containment spray performance under severe accident conditions. In: Proceedings of 8th European Review Meeting on Severe Accident Research (ERMSAR), Warsaw, Poland, 2017
38. Freitag M, Gupta S, Beck S, et al. Experimental and analytical investigations of aerosol processes—wash-out and wash-down. Nuclear Science and Engineering, 2019, 193(1 – 2): 198–210
39. Kühnel A, Fischer K, Langer G. Test TH-19 in the THAI facility on the performance of spray systems. Report: BT-70084–1, 2006
40. Gupta S, Langer G. Experimental research on hydrogen deflagration in multi-compartment geometry and application to nuclear reactor conditions. Nuclear Engineering and Design, 2019, 343: 103–137
41. Freitag M, von Laufenberg B, Colombet M, et al. Measurements of the impact of carbon monoxide on the performance of passive autocatalytic recombiners at containment-typical conditions in the THAI facility. Annals of Nuclear Energy, 2020, 141: 107356
42. Cheng L, Woo K S, Ishii M, et al. Suppression pool mixing and condensation tests in PUMA facility. In: Proceedings of 14th International Conference on Nuclear Engineering, Miami, USA, 2008
43. Laine J, Puustinen M. Thermal stratification experiments with the condensation pool test rig. Report: NKS-117 ISBN 87–7893–178–9, 2006
44. Balewski B, Gupta S, Fischer K. Water flow with bubble columns-Boiling Water Reactor experiments WH-7 to WH-15. Technical Report: 1501361-WH-7–15-FB/TR, 2011
45. Paul D D, Flanigan L J, Cunnane, J C, et al. Radionuclide scrubbing in water pools. Report: EPRI NP-4154-L, 1991
46. Ouallal M, Leyer S, Gupta S. Literature survey of droplet entrainment from water pools. Nuclear Engineering and Design, 2021, 379: 111188
47. Schmidt E W, Gupta S, Freitag M, et al. Wet resuspension of insoluble material from a boiling sump. In: Proceedings of the International Conference on Nuclear Engineering: ICONE, Chiba, Japan, 2015
48. Bunz H, Koyro M, Propheter B, et al. Resuspension of fission products from sump water. Final Report: EUR 14635 EN, 1992
49. Cosandey J O, von Rohr P R. Entrainment of soluble and non soluble tracers from a boiling water surface. Nuclear Engineering and Design, 2001, 208(1): 87–97
50. Freitag M, Schmidt E, Colombet M, et al. Aerosol retention in water pools-Pool Scrubbing. Technical Report: 1501547-FB/TR-WH25–27, 2018